Investigation of the Effect of Load Duration on Swelling Pressure and Preconsolidation Stress in Oedometer Testing on Søvind Marl

Master Thesis

Ma Dimphna Sumaoy

Aalborg University
Department of Civil Engineering

The Faculty of Engineering and Science
Study Board of Civil Engineering
Thomas Manns Vej 23
9220 Aalborg Øst
http://www.aau.dk

AALBORG UNIVERSITY
STUDENT REPORT

Title:
Investigation of the Effect of Load Duration on Swelling Pressure and Preconsolidation Stress in Oedometer Testing on Søvind Marl

Theme:
Master Thesis

Project Period:
September 2018 - December 2018
September 2019 - Febuary 2020

Student(s):
Ma. Dimphna Sumaoy

Supervisor(s):
Lars Damkilde
Søren Dam Nielsen
Benjaminn Nordahl Nielsen

Copies: 1

Page Numbers: 90

Date of Completion:
Febuary 10, 2020

Contents

Preface

This thesis "Investigation of the Effect of Load Duration on Swelling Pressure and Preconsolidation Stress in Oedometer Testing on Søvind Marl" is the product of a long master project carried out in the period of September 2018 to December 2018 and continued in the period of September 2019 to Febuary 2020 at Department of Civil Engineering, Aalborg University, Denmark. It reports on the investigation of the influence of load duration on soil deformations on a highly plasticity and highly overconsolidated clay - Søvind Marl.

I would like to thank my formal AAU supervisor Professor Lars Damkilde for providing feedback throughout this project. I would also like to express my deepest appreciation to my external supervisors Benjaminn Nordahl Nielsen and Søren Dam Nielsen for always taking time to come at AAU for meetings, to guide and counsel me. All my supervisors time and work is much appreciated.

I also wish to thank the technical staffs at AAU Geotechnical Laboratory, Engineer Constructor Anette Næslund Pedersen and Engineer Assistant Morten Lars Olsen for their guidance during the experimental tests and for their help and effort in checking my oedometer tests in the laboratory while i am away during my maternity leave.

Finally, i would like to thank my family and friends for all the unconditional love and support in this very intense academic year.

Aalborg University, Febuary 10, 2020

Ma Dimphna Sumaoy
<msumao15@student.aau.dk>

List of Symbols

Greek Symbols

γ	Bulk density
γ_w	Water density
$\Delta\varepsilon$	Increase in strains
$\Delta\varepsilon_c$	Increase in consolidation strains
$\Delta\varepsilon_{\alpha\varepsilon}$	Increase in creep strains
$\Delta\sigma$	Total stresses
$\Delta\sigma'$	Increase of effective stresses
Δu	Increase of excess pore pressure
δ	Displacement
δ_1	Axial displacement 1
δ_2	Axial displacement 2
δ_t	Displacment from the frame
ε	Strains
ε^E	Engineering strains
ε^N	Natural strains
ε_c	Consolidation strains
ε_{creep}	Creep strains
ε_{tot}	Total strains
ε_{tot}^{end}	End point of total strains
σ	Axial stresses
σ'	Vertical effective stresses
σ'_k	Reference stresses
σ'_m	Vertical effective mean stresses
σ'_{pc}	Preconsolidation stresses
σ_s	Swelling pressure
σ'_{v0}	In-situ stresses

Latin Symbols

A-line	Lower limit line
C_c	Compression index
C_r	Recompression index
$\Delta\varepsilon_{\alpha\varepsilon}$	Increase in secondary compression index
c_v	Coefficient of consolidation
e	Void ratio
H_0	Initial sample height
I_p	Plasticity index
k	Coefficient of permeability
LIR	Load increment ratio
m_0	Initial mass
m_{pl}	Mass of the lower pressure head
m_u	Mass of the upper pressure head
m_{pu}	Mass of the filter
m_r	Mass of the oedometer ring
m_{total}	Total mass
M	Consolidation modulus
NC	Normally consolidated soil
OCR	Overconsolidation ratio
OC	Overconsolidated soil
P	Axial load
T	Dimensionless time
t	Measured time
t_A	Guessed time or time before creep started
U	Degree of consolidation
u	Pore pressure
U-line	Upper limit line
$USCS$	Unified soil classification system
w	Water content
w_L	Liquid limit
w_P	Plastic limit

Summary

This thesis focuses on the investigation of the effect of load duration on preconsolidation stress and swelling pressure in oedometer testing on Søvind Marl. This type of clay has a high plasticity, highly overconsolidated and highly calcareous. In addition, it has a fissured structure that influenced the stiffness of the clay. These fissures were caused by the failure of the clay due to the load and unload of glaciers. The geological description of Søvind Marl is presented in Chapter 2. As settlements and swelling are expected to cause damage to structure on these types of clays, it is of utmost important to determine the correct soil deformation characteristics on these clays by performing oedometer tests.

In practice, most oedometer tests are performed as incremental loading test with 24hr measurements in order to save time. However, the more correct evaluation of oedometer test should consider the time for swelling to occur after the sample has been saturated and allows all settlements to be completed. Otherwise measurements of swelling and settlements on soil can be underestimated. Therefore, the main goal of this project is to investigate the effect of load duration by letting the sample to fully consolidate and obtain the exact pressure that can resist swelling during oedometer testing and compare it to the traditional 24 measurements.

Two samples (Test01 and Test02) were tested in 24hr load step test and two samples (Test03 and Test04) were tested in 14day load step test. All the samples are in the same height of 35 mm and diameter of 35 mm. Before the oedometer started, a classification test was made on these samples in order to determine the initial condition of the soil. Here the water content, liquid limit, plasticity index, bulk density and void ratio were obtained and are presented in Chapter 3. Furthermore, in this chapter the method of oedometer test is discussed. Figure 1 illustrates the stages of the investigation study.

In stage 1, all the tests are performed by constant volume test to measure the swelling pressure. The swelling pressure in short duration tests (Test01 and Test02) was measured after 24 hours while Test03 and Test04 were tested for approximately 4 months until the exact swelling pressure was reached. The interpretation of the results are discussed in Chapter 5. It is found that the exact swelling pressure (pressure at which swelling stopped) was

obtained at approximately 3 months of testing. Hence, 24hr measurement underestimated the said parameter.

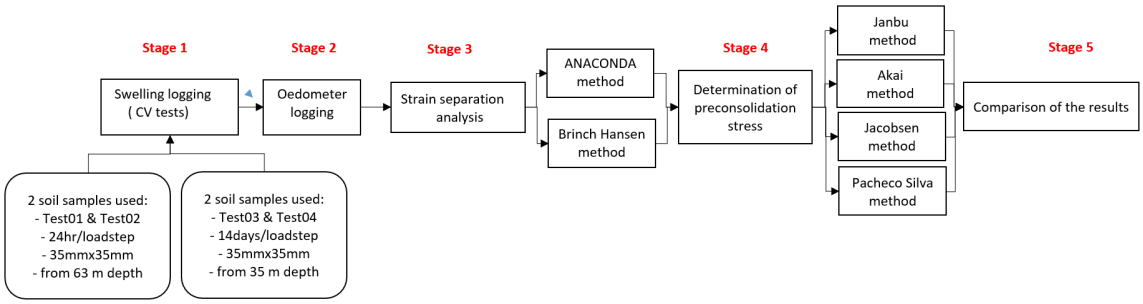

Figure 1: Stages of the investigation study in this project.

Once the swelling pressure was obtained, the oedometer test was carried out. The results are presented in Chapter 3. Here the stress-strain curves of 24hr load step tests is greater than the stress-strain curves of 14day load step tests, which was not expected. It is argued in Chapter 5 that this was due to fissured structures present in the samples from 63m depth (used in 24hr load step tests). Previous research found that the spacing between fissures widens with depth. These fissures were forced to be closed at lower stress level causing large strains during the first and second load step in 24hr load step tests samples.

After the oedometer tests were completed, the total strains (each step) were separated using ANACONDA and Brinch Hansen's method (stage 3). In Chapter 5, the results were interpreted and compared. It was found that the two methods gives more accurate and certain results if the oedometer tests are performed with longer load duration. Both methods determined that the consolidation was completed at approximately 2 days. However, in 24hr measurements, there was a variation of the results. Both methods determined that the complete consolidation was reached earlier after 2-8 hours.

Next, the isolated consolidation strains results in each load step were used in an analysis to determine the preconsolidation stress using different methods (Janbu, Akai, Jacobsen and Pacheco Silva) in stage 4. The data analysis using these methods is presented in Chapter 4 and the results are compared in Chapter 5 (stage 5). In this thesis, the lower bound of the preconsolidation stress was found approximately 500 kPa while the upper bound preconsolidation stress was found in a range of approximately 4700 kPa to 9200 kPa. However, there was a variation of preconsolidation stresses obtained by Jacobsen's method. The 24hr measurement tests underestimated the preconsolidation stress by 30-36% based on this method.

Overall, the investigation in this project found that 24hr measurements in oedometer testing is not sufficient for these types of clays as it can lead to underestimation of soil deformations.

Chapter 1

Introduction

Søvind Marl is a highly calcareous, highly fissured, extremely plastic and highly overconsolidated clay. It is one of the types of plastic clays that can be found in some regions of Denmark which has challenged geotechnical engineers for decades. Figure 1.1 illustrates the city of Aarhus Denmark (inside the black circle) where Eocene deposits such as Søvind Marl can be found.

Figure 1.1: Eocene deposits (marked with dark band) found in Denmark and in north-western part of Zealand. Søvind Marl is a Eocene deposits found in Aarhus Denmark (indicated by the black circle). (Grønbech (2015)).

These plastic and expansive clays can cause large settlements or uplift of structures both during the construction phase and over the lifespan of the finished construction. Some examples of this is what happened at Skive Museum back in the 1940's, where the museum rose 10 *cm* in a few years after construction. Recently, the Old Little Belt Bridge has sunk 75 *cm* where Banedanmark (which maintains most of the Danish railway network) spent 200 million Danish kroner (27 million euros) to save the bridge (Simonsen (2017)).

As Søvind Marl is considered as one of the challenging soils to build on, it is very important to determine the geotechnical properties of this clay before any construction, in order to design an effective building foundation. One way to do it is to conduct oedometer tests of undisturbed clay soils recovered during the site investigation and this method is used in this thesis.

Oedometer tests also referred to as consolidation tests are used for measurement of soil deformations vs. one dimensional load. These tests are used to determine the expected swelling and settlement of the soil for a given load. The perfect oedometer test needs to have a duration which allows all settlements to be finished. However, as this is time consuming, a compromise is often 24hr measurements and has been traditionally performed. The 24 hour duration may not be sufficient for high plasticity clays such as Søvind Marl (depending on the height of the sample, the load increment ratio (LIR) applied and the type of drainage being used in the test) because Søvind Marl is a highly overconsolidated clay. Overconsolidation means that the clay has experienced a high load prior to the load during the test, and there has a high preconsolidation stress. This means that during oedometer testing, the clay will consolidate and compress at a relatively slow rate. In addition, the plasticity of the clay makes it more difficult to dissipate the pore water pressure during the test. Therefore oedometer tests on this type of clay should consider including a duration of time for swelling to occur after sample saturation and let full consolidation be reached. Otherwise measurement of soil deformation can be underestimated.

In this thesis, the effect of load step duration during oedometer testing will be investigated on Søvind Marl, by considering geotechnical parameters such as preconsolidation stress and swelling pressure. This will be done by conducting a series of oedometer tests in 24hr and 14day load steps. Based on that, a comparison will be performed. The purpose of this study is to give insight into the behaviour of overconsolidated high plasticity clays by investigating the effect of letting these clays to fully consolidate during testing compared to the traditional and economically preferable 24hr measurements.

1.1 Theory

This section briefly summarises the theory of consolidation that is used in the analysis to determine the preconsolidation stress and the concept of swelling. In addition, a brief

description of the procedure for performing an oedometer test is also presented.

1.1.1 Consolidation

Consolidation is the dominant component of the total settlement calculation, particularly in Normally Consolidated fined grained soil, as it produces the largest settlement of structures. The total settlement consists of three components: initial settlement (elastic deformation and fully recoverable), consolidation (plastic deformation and only partially recoverable) and creep (plastic deformation and unrecoverable). The initial settlement occurs over a short period of time (normally ends during the construction phase).

The consolidation process is briefly described using a simplified system analog to the clay layer, which is shown in Figure 1.2 and Figure 1.3. In this analog, a valve acts as the permeability of the clay, water acts as the water in the clay while the spring acts as the clay skeleton. At stage (a) the initial condition of the container is shown. Here the container is completely filled with water, and the valve is closed. Hence the clay is fully saturated. During stage (b) a vertical stress is applied, but the valve is still closed. Since the valve is closed the water cannot dissipate through the valve, and an excess pore pressure develops equal to the load increased. The excess pore pressure instantly increases and this will cause the total stress to increase as well, whereas the effective stress is unchanged. When the valve is open at stage (c), the stress (load) is carried partly by the water and partly by the spring. The water slowly dissipates from the valve causing the excess pore pressure to gradually decrease and with time the pore pressure dissipates. The stress (load) is then carried by the spring causing the effective stress to increase. When the excess pore pressure Δu is fully dissipated ($\Delta u=0$) at stage (d), the stress is entirely carried by the spring. At this stage the consolidation process ends. However, the small settlement continues due to the rearrangement of the grains under constant effective stress. This settlement is called creep.

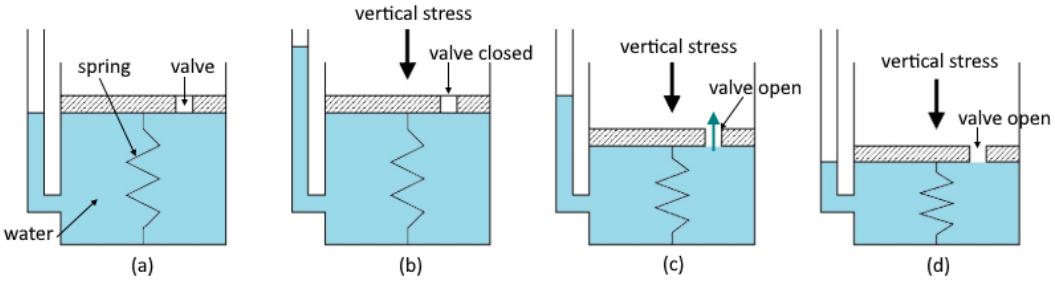

Figure 1.2: Consolidation process a spring analog. (a) Initial condition (no stress applied). (b) Development of excess pore pressure (c) Dissipation of excess pore pressure. d.) Excess pore pressure is fully dissipated (end of consolidation). Wikipedia (2013) edited.

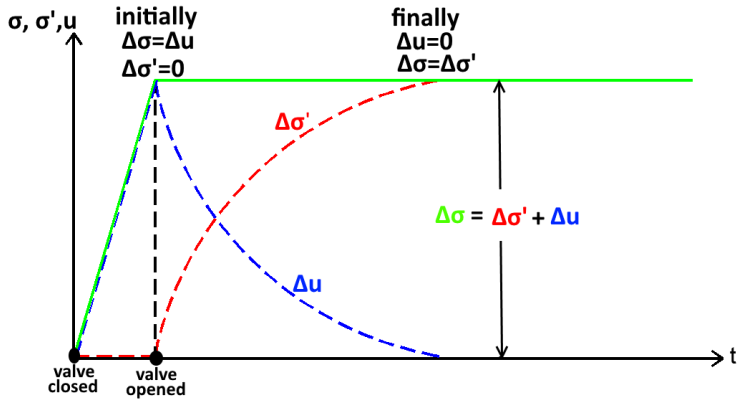

Figure 1.3: Consolidation process in Figure 1.2. When the valve is closed, the excess pore pressure Δu increases causing the total stress $\Delta\sigma$ to increase, whereas the effective stress $\Delta\sigma'$ is unchanged. When the valve is opened, the excess pore pressure Δu gradually decreases (pore water slowly dissipates) and effective stress $\Delta\sigma'$ gradually increases (clay skeleton carries the stress (load)). With time, the excess pore pressure Δu=0 (consolidation ends) and effective stress $\Delta\sigma'$= total stress $\Delta\sigma$.

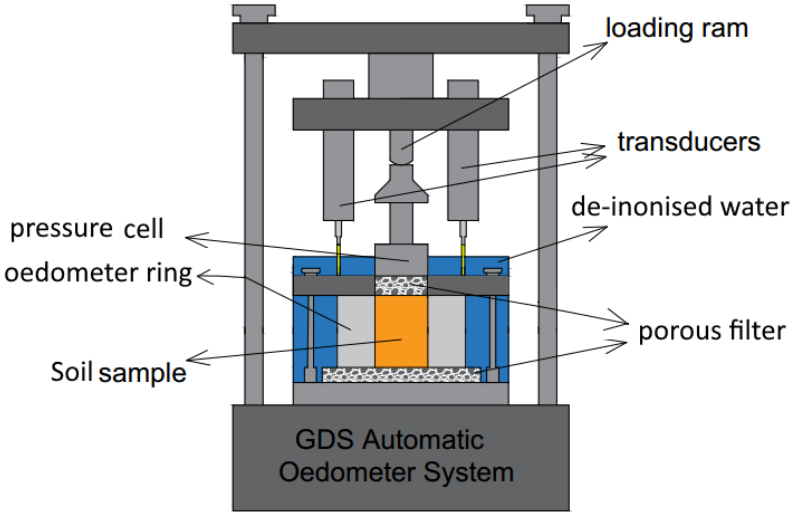

Figure 1.4: Schematic diagram of an oedometer test apparatus.

The investigation of consolidation behavior can be done by conducting an oedometer test. Figure 1.4 shows a schematic diagram of oedometer test apparatus. Here the sample is confined in oedometer ring and immersed in de-ionised water. The test can be performed as either an incrementally loaded or a continuously loaded test. Conventionally, an oedometer test procedure with incremental loading is performed. The sample is subjected to a series of increasing load increments from the frame and through the loading ram with a duration of 24 hours for each stage. This duration was suggested by Terzaghi (1925) and

was traditionally applied since then. During the test, each increment causes an increase in pore pressure which dissipates in the porous filter above and below the soil sample. The final (total) settlement and settlement rate are measured by the transducers and recorded during each loading increment.

When interpreting an oedometer test, only the consolidation strains will be used in the analysis of the results. Since consolidation and creep run simultaneously, it is necessary to separate the total strains and isolate the consolidaton strains. This can be done by using different strain separation methods. Several of these methods are included in the thesis, which are the ANACONDA and Brinch Hansen's method. These are described in Chapter 4. In order to not wrongfully separate the total strains, it is important that the full consolidation of the soil takes place in each load step, prior to starting a new step.

Moreover, one of the significant consolidation properties that is determined in oedometer testing is the preconsolidation stress σ'_{pc}. It is the maximum vertical effective stress that the soil has sustained in the past. Usually larger stress in the past is due to the weight of glaciers and the weight of younger layers that have subsequently been removed by erosion. If the preconsolidation stress σ'_{pc} is known, the overconsolidation ratio OCR is determined. OCR is the ratio of σ'_{pc} over the in-situ stress σ'_{v0} of the soil. If the overconsolidation ratio is equal to 1, the soil is normally consolidated NC (σ'_{v0}=σ'_{pc}) and if the overconsolidation ratio is greater than 1, the soil is overconsolidated OC (σ'_{v0}<σ'_{pc}). Normally consolidated soils deform more than overconsolidated soils when the vertical stress in the soil increases. This is the reason why preconsolidation stress is an essential parameter to be determined in order to know which soil can be loaded without producing large settlements.

1.1.2 Swelling clay

Swelling clays or expansive clays are ones that swell in volume when water is introduced as shown in Figure 1.5. Clays containing smectite mineral are characterized as expansive clays.

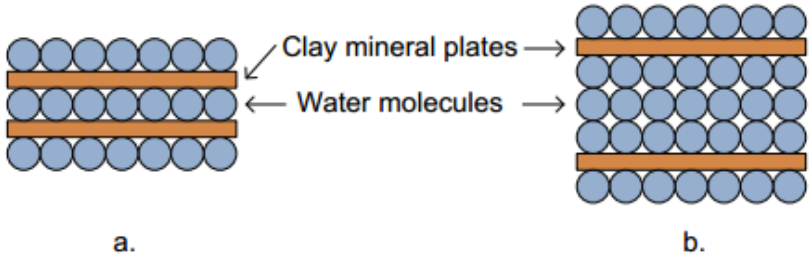

Figure 1.5: a. Before swelling. b. After swelling. The water molecules are absorbed by the clay minerals causing an increase in volume that causes the clay mineral plates to move further apart. Kaufmann (2010)

One of the main instances when swelling occurs is when the pressure in the clay decreases e.g. excavation work. The decrease of pressure can be seen in Figure 1.6. The initial condition before excavation can be shown in Figure 1.6(a). Right after the excavation (b), the total stress decreased as the pore water pressure decreases, whereas the effective stresses are unchanged. After some time (c), the pore water from the surrounding soil is absorbed by the clay minerals and therefore the soil starts to swell. As differences in pressure seek to balance and since the total stress is unchanged, the effective stress decreases to match the increase of pore water pressure.

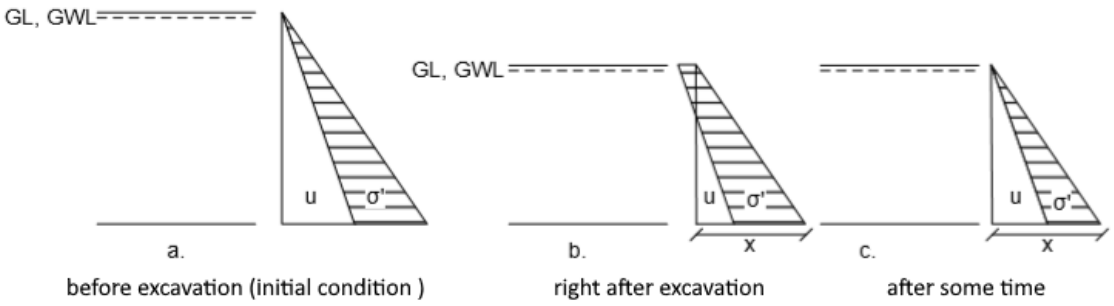

Figure 1.6: a. The initial conditions before excavation. b. Right after excavation. There is a decrease in total stresses which is seen as a decrease in pore pressure. Here the effective stresses are unchanged. The soil has not reached equilibrium or adapted to the change in GWL and GL. c. After some time, the clay will start to swell. It will absorb water from the surrounding soil and reach hydrostatic pressure again. Since the total stresses should remain the same, the effective stresses decrease so equilibrium can be reached once again. LG is ground level and GWL is ground water level.(Kaufmann (2010)).

In Denmark, swelling clays (expansive clays) are abundant. This is due to the large content of smectite mineral present on these clays. This type of clay can cause severe damage on structures by settling (as it gets dry) and lifting (as the clay minerals absorb the water). It was estimated in the United States of America that the cost of damage to structures on these expansive clays exceed the combined cost of all damage caused by any natural disasters such as earthquakes, tornadoes, hurricanes and floods (Holtz (1983)).

The swelling potential of clay can be determined by the use of oedometer tests which is commonly used due to its simplicity, and most geotechnical engineers are familiar with this testing method. One of the common types of tests performed to measure the swelling pressure is the constant volume test (which is used in this thesis). In this test the soil sample is prevented from swelling during the saturation and because swelling is prevented, the pressure will generate instead. This pressure is the measured swelling pressure. In order to obtain the correct measurement of swelling pressure, it is therefore important to consider the time for swelling to occur after the soil is saturated in order to determine the exact swelling pressure.

1.2 Problem statement

What is the effect of load duration on swelling pressure and preconsolidation stress in oedometer testing on Søvind Marl?

Figure 1.7 shows an example of a variation of swelling pressure measured with time from a constant volume test. Figure 1.7(a) shows the initial condition before the specimen (in brown) is saturated. When the water is poured on to the cell (b in the left), the specimen starts to absorb the water and attempt to swell. The vertical stress is adjusted to prevent the development of the strains (strains=0). Figure 1.7(b in the right) shows the measured swelling pressure after 24 hours. With time (c), when the curve converges in $t - \sigma$ (c in the right), the stress that is required to prevent swelling is the correct and precise swelling pressure.

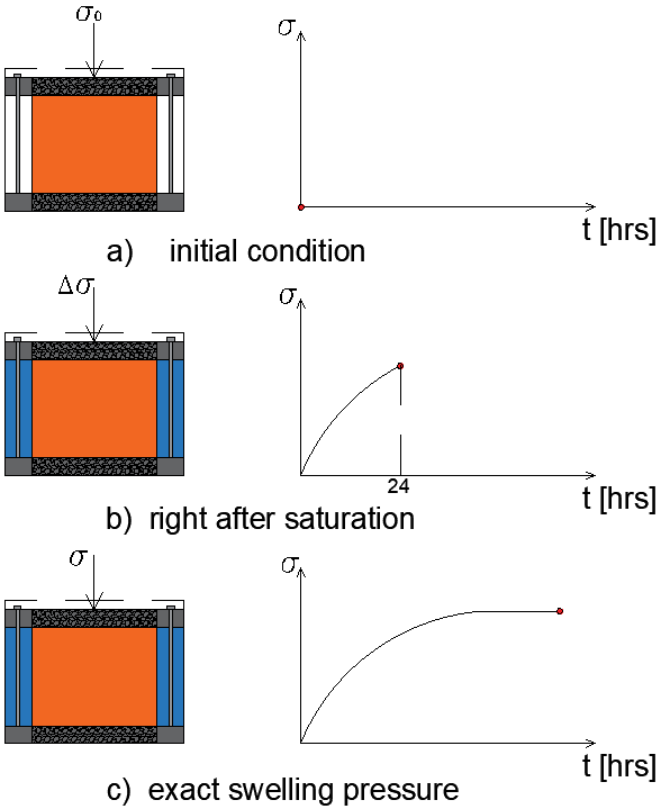

Figure 1.7: a) The initial condition before the water is poured in the cell. b) The water (in blue) is added. The specimen (in brown) starts to absorb the water and attempt to swell. The vertical stress is adjusted to prevent the development of the strains. In the left shows the swelling pressure measured after 24 hrs. c) With time, when the curve converges in $t - \sigma$ (c in the right), the correct and precise swelling pressure is obtained.

Moreover, figure 1.8 shows the construction of continuous stress vs. consolidation strain curves obtained in oedometer testing. The stress vs. consolidation strain curve is needed in order to see the soil deformation due to the increase of the load applied. However, during testing the total strains are measured. Therefore a series of load steps are needed, where each load step is fully consolidated. Figure 1.8(a) shows the loading diagram in oedometer testing in each load step with a constant load. In each load step, the total strains are measured shown in $\log(t) - \varepsilon$ plot (b). As only the consolidation strain will be used in the deformation analysis, the consolidation strains are isolated in (b) and plotted in stress vs. consolidation strain curve (c). Assuming that ε_{100} is where consolidation is completed while ε_{24} is the strain measured after 24 hours. It can be seen that the 24hr measurement (c) shows less deformation as the consolidation was not completed.

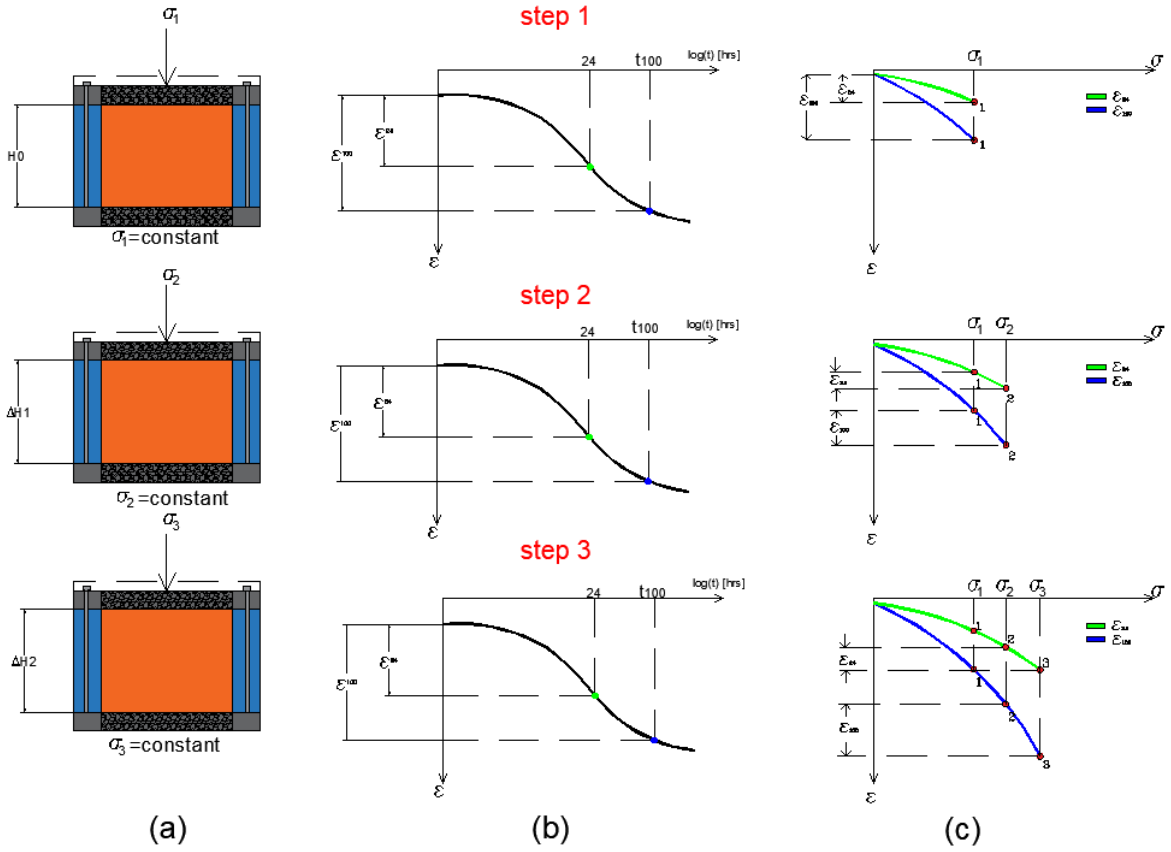

Figure 1.8: a) Shows the loading diagram in oedometer testing in each load step with a constant load. b) Shows the outcome of each load step with a constant load plotted in $\log(t) - \varepsilon$ graph. Assuming that ε_{100} is the complete consolidation while ε_{24} is the strain measured after 24 hours. c) ε_{100} and ε_{24} from (b) are isolated and plotted in stress vs. consolidation strain.

To verify if the 24hr measurements underestimated the soil deformation parameters de-

scribed above, part of the thesis focuses on the investigation of the effect of load step duration on preconsolidation stress in oedometer testing by conducting four oedometer tests with two different load step durations. Two samples were tested in 24hr load step test and two samples were tested in 14day load step test.

The soil sample that was used in the investigation is an extremely high plasticity, highly calcareous and highly fissured clay - Søvind Marl. The clay is overconsolidated due to weight of glaciers and younger soil layers that are now eroded, thus this clay has a high component of creep up to 1% (Grønbech et al. (2013)). This type of soil can be found in Aarhus Denmark which takes more than 24 hours to fully consolidate the soil. However, as 24hr measurement in oedometer testing is a time and cost- effective process, this load step duration is preferred by many engineers and had been traditionally used.

In addition, the effect of load duration on swelling pressure σ'_s measurement is also investigated on this swelling clay. Søvind Marl is considered as extremely high plasticity clay due to the large content of smectite mineral. In this thesis the swelling pressure was measured using constant volume test as it is important to measure the swell pressure at the same void ratio (volume) as is the case in-situ (Okkels and Hansen (2016)). Two samples were used to measure the swelling pressure after 24 hours while two samples have been tested in a sufficiently long period that the equilibrium swelling was reached.

1.3 Methodology

The order of approach in this thesis is illustrated in Figure 1.9. This is utilised to achieve the final goal of the investigation of the effect of load duration on swelling pressure and preconsolidation stress in oedometer testing on Søvind Marl.

Two samples (Test01 and Test02) were tested in 24 hr load step test and two samples (Test03 and Test04) were tested in 14day load step test. The swelling pressure was measured before applying the first load step in consolidation test in four samples. In short duration test, the swelling pressure was measured after 24 hours while in the long duration test, it took approximately four months for the swelling pressure to be determined. Several methods were used in this thesis to assess the prediction of the consolidation and creep strains. These are the ANACONDA and Brinch Hansen's method. The total consolidation strain results in each load step were separated and the consolidation strain was isolated for further calculation. Furthermore, σ'_{pc} was determined using different methods; Akai (1960), Janbu (1969), Pacheco Silva (1970) and Jacobsen (1992).

Finally, the results are compared and the effect of different load duration on sweling pressure and preconsolidation stress on Søvind Marl was investigated.

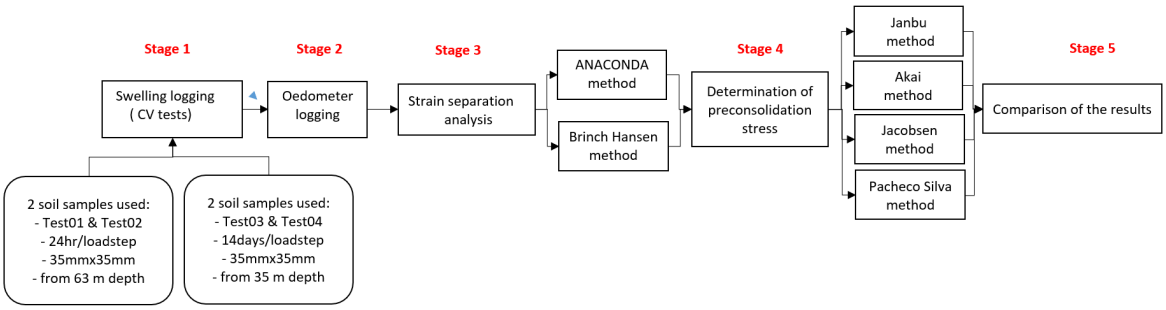

Figure 1.9: Flow chart of the order of calculation flow in this thesis. The soil samples' test names, duration of the load step, size of the specimens used and the depth it was taken used in short-term tests (left) and long-term tests (right) are split into two. In stage 1 from the left, all the soil samples are performed by constant volume test to measure the swelling pressure. The swelling pressure in short-term tests (Test01 and Test02) were measured in 24 hrs while Test03 and Test04 were saturated fro approximately 4 months until the exact swelling pressure was reached. In stage 2, the oedometer logging starts where all the soil specimens were incrementally loaded by 15 load steps. In stage 3 the total strain in every load step was separated using ANACONDA and Brinch Hansen's method. The isolated consolidation strains results in each load step were used in the analysis to determine the preconsolidation stress using different methods (Janbu, Akia, Jacobsen and Pacheco Silva) in stage 4. Finally in stage 5, the results were compared.

1.4 Overview of the thesis

The overview of the chapters of this thesis are shortly describe below.

- Chapter 2 In this chapter the geological description of studied Søvind Marl is presented. Here the historical background of Søvind Marl is shortly described. It also presents the soil classification of the four samples.
- Chapter 3 This chapter covers the soil data and test method of oedometer test. It also describes the initial condition of the soil before the test is performed. Furthermore, the outcome of the oedometer tests is illustrated.
- Chapter 4 Contains the data analysis. The analysis consists of two stages: the strain separation analysis and preconsolidation stress ananlysis. The results of the four samples after the data was analysed are presented in this chapter.
- Chapter 5 This chapter contains the interpretation of the results and discussion of effects of the load duration used in oedometer testing on Søvind Marl in this thesis, regarding the results determined in Chapter 4.
- Chapter 6 In this chapter, the conclusion of the investigation is presented as well the as the recommendations for future investigation.
- Appendix A Presents the description of consolidation parameters.

- Appendix B Illustrates the outcome of $\log(t) - \varepsilon$ in every load step for all the samples. The curves are plotted in one graph (each step) in order to see the effect of the curve when an oedometer test is performed in 24hr and 14day load step duration.
- Appendix C Contains the plots of strain separation analysis results in all test samples. The parameters determined in the methods used are summarised in a table.
- Appendix D The plots of preconconsolidation stress analysis results using various methods in all test samples are presented in this appendix.

Chapter 2

Geological description

Søvind Marl is one of Denmark's most complicated soil to build on and it is very important to understand why. In this chapter, the geological background of this type of clay is presented.

In addition, the location of the studied clay, boring records and the results of the classification of soil of four samples are covered in this chapter as well. The soil classification made on these samples was not tested by the author itself. The soil classification results presented in this chapter were provided from AAU. The liquid limit ω_L and plasticity index I_p of the soil specimens are determined from Fall Cone method based on (DS 2004b) as it is the preferred method than the Casagrande cup method Grønbech (2015). Fall Cone method is widely used and the accepted standard in obtaining the liquid limit. As the main focus in this study is solely on oedometer testing, the Fall Cone test method is not covered in this study.

2.1 Geoglogical background

The information in this section is summarized from the original source referred from Grønbech (2015) and Geoviden (2010).

The geological time of tertiary period consists of two different intervals. These are the Paleogene period (which lasted from 66 million to 23 million years ago) and Neogene period (which lasted from 23 million years ago and the present). Paleogene period are divided into four eras: Danien, Paleocene, Eocene and Oligene era. The geological time scale of these Paleogene deposits are shown in Figure 2.1.

The tertiary deposit, Søvind Marl was deposited during the middle Eocene period (which lasted from 47.5 million to 38 million years ago) to late Eocene period (which lasted from

38 million to 33.9 million years ago) as shown in Figure 2.1 (inside the box). Only the geologic and climatic change in this era will be focus in this section.

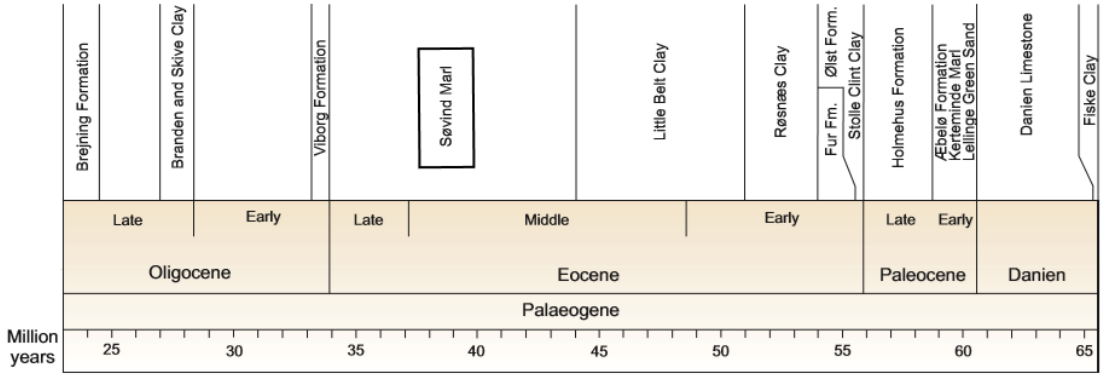

Figure 2.1: The geological time scale of these Paleogene deposits (Grønbech (2015)). Paleogene period are divided into four eras: Danien, Paleocene, Eocene and Oligene era. Søvind Marl (inside the rectangle box) was deposited in the middle Eocene period (which lasted from 47.5 million to 38 million years ago).

During this period, the global climate was remarkably warmer containing relative high sea levels. At that time, Denmark was covered by a large ocean with tertiary sediments mainly consists of limestone (which became a fine grained clay due to the rise of temperature) and fat clays which are all marine deposits. These sediments were slowly filled up over the course of million years.

Coinciding with this, several volcanic eruptions took place causing the ashes to spread over most of Northern and Central Europe and ended up in the ocean alongside the tertiary sediments. These ashes was chemically transformed into clay minerals later on. These clay minerals are smectite, kaolinite and illite. After the major volcanic eruptions, the Islandic hotspot cooled during this era which have caused the land to settle due to its weight which has subsequently been removed by erosion. These events have resulted a tearing and developed fissures formation on the clay.

In previous investigation of Søvind Marl, Grønbech (2015) determined the mineral composition of the said clay that was retrieved from Aarhus Harbour (similar location of studied Søvind Marl used in this thesis) using X-ray powder diffraction. Søvind Marl based on this area was recorded more than 60 m. It was found that this clay has clay mineral composition up to 95% with 35-45% of the total sediment soil sample at every depth consists of smectite.

In addition to that, the calcite composition was also found. Figure 2.2 shows the variations of calcite content of 5 borings (labelled 7, 8, 9, 10 and 11) in the same location (Aarhus Harbour). The test samples used in this project were rest of the samples used in Grønbech (2015) experiments from boring 11 at 35 m and 63 m depth. Based on the results, calcite

level was measured 15 to 30% in the first 15 m and beyond 25 m, the calcite percentage slightly increases to 40%. However, from 50 m, the calcite percentage declined to 5 to 30% and almost calcite free as it reach to 70 m. Moreover, Grønbech (2014) also found that there is a high correlation between calcite content and plasticity index on Søvind Marl. It is evidently shown in Figure 2.3 that $CaCO_3$ and I_p are strongly related to each other. An increasing calcite content level shows a decreasing level of clay's plasticity.

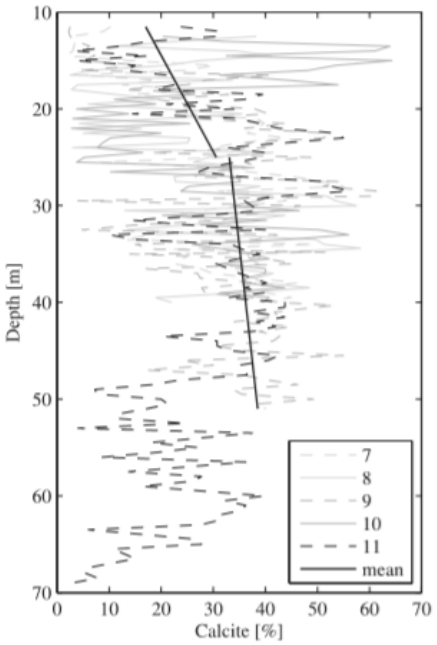

Figure 2.2: Variation of calcite content of Søvind Marl after Grønbech (2014) experiments. The test samples used in this project were rest of the samples used in Grønbech (2015) experiments from boring 11 at 35 m and 63 m depth.(Grønbech (2014))

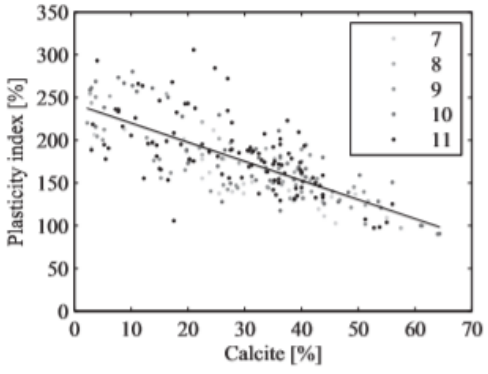

Figure 2.3: Correlation between calcite content and plasticity index on Søvind Marl after Grønbech (2014) experiments. An increasing calcite levels are associated with decreasing plasticity.(Grønbech (2014))

2.2 Studied Søvind Marl

The studied Søvind Marl is based on the boring records used in this thesis. The borings (LH830 and LH900) were retrieved from Aarhus Harbour, Denmark shown in Figure 2.4 with a red pin inside the red box. The segments of boring records of LH830 and LH900 in depths of 35 m and 63 m, respectively, are shown in Figure 2.6 and Figure 2.5. As described in previous section, these soil samples that was used in this thesis are approximately 46 million years old.

Figure 2.4: Location of the studied Søvind Marl. The boreholes were retrieved in Arhus Harbour which is shown inside the red box. Google map (2019) edited.

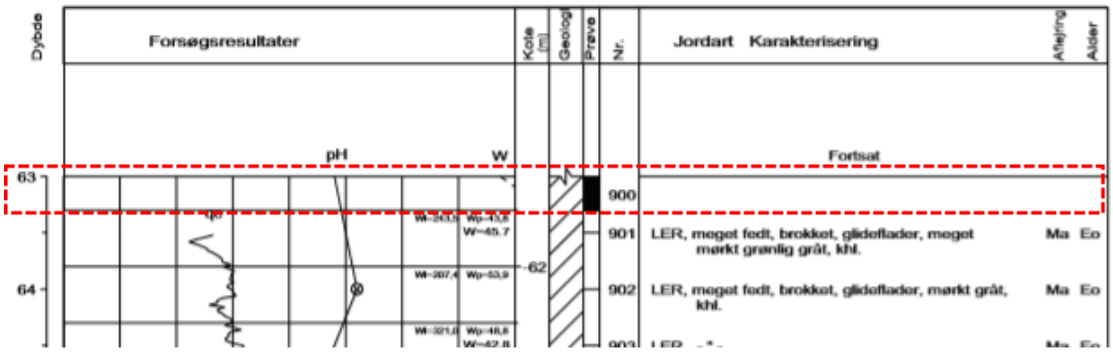

Figure 2.5: Boring LH900 used in Test01 and Test02 (24hrs/load step tests) at 63 m. Grønbech (2014)) edited.

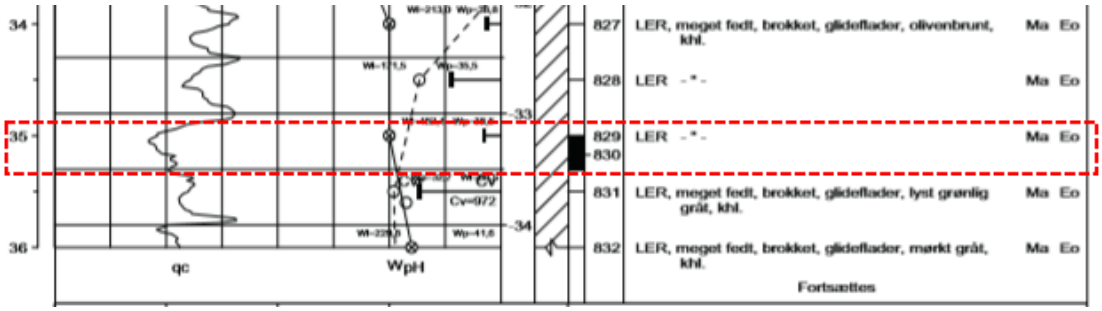

Figure 2.6: Boring LH830 used in Test03 and Test04 (14days/load step tests) at 35 m. Grønbech (2014)) edited.

The sample from boring LH830 (from 35 m depth) in Test03 before (left) and after (right) the oedometer test can be seen in Figure 2.7. During the preparation of the sample, the fissures surface of Søvind Marl was visible. The fissures of Søvind Marl were developed during the glacial time where the clay was loaded and unloaded. During the glacial melts and erosion (force was unloaded), this leads the clay swell which results the tearing of the clay and thus fissures are formed Grønbech (2015). The effects of these fissures can also be shown in Figure 2.7 after the consolidation test where the sample was cutted into half. Here it can noticeably seen that the fissures are closed (dark color of lines).

Figure 2.7: Sample from boring LH 830 used in Test03 before (left) and after (right) the consolidation test. (AAU lab)

2.3 Soil classification

The classification of Søvind Marl can be seen in Table 2.1. The liquid limit ω_L and plasticity index I_p of the samples are determined from the Fall Cone method based on (DS 2004b) as it is the preferred method than the Casagrande cup method Grønbech (2015).

Test	water content w [%]	liquid limit w_L [%]	plastic limit w_P [%]	plasticity index I_p [%]	bulk density γ [kN/m^3]
Test01	42.80	203.26	45.6	157.7	17.28
Test02	44.56	192.86	42.10	150.8	17.69
Test03	41.63	158.32	46.7	111.6	17.98
Test04	40.15	152.69	44.2	108.4	17.98

Table 2.1: Soil classification of the studied Søvind Marl.

In order to determine the soil plasticity, the Casagrande plasticity chart is use where the liquid limit w_L is plotted against and the plasticity index I_p. Based on Table 2.1, the liquid limit and plastic index are extremely high. This is then expected as the clay was determined extremely plastic in the previous research of Grønbech et al. (2014) and made it to extend and updated the Casagrande chart from four into six categories. The plot of w_L against I_p according to the updated plasticity chart can be seen in Figure 2.8 and the categories are presented in Table 2.2.

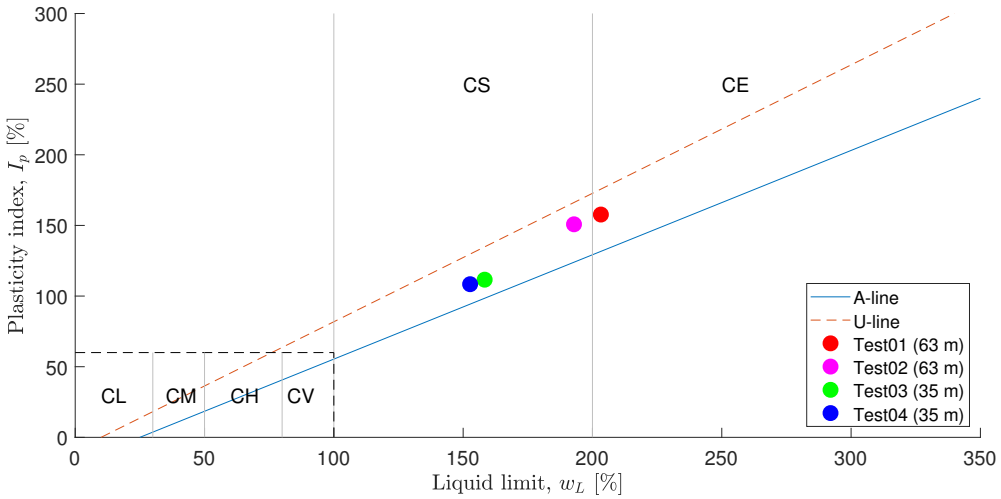

Figure 2.8: Plasticity chart (updated). The dashed-line which corresponds w_L (0-100) and I_p (0-60) is the original Casagrande chart. A-line define as lower limit line and U-line define as upper limit line.

Categories	liquid limit w_L [%]	USCS
Low plasticity clay	<30	CL
Medium plasticity clay	30-50	CM
High plasticity clay	50-80	CH
Very high plasticity clay	80-100	CV
Super high plasticity clay	100-200	CS
Extremely high plasticity clay	200-350	CE

Table 2.2: Classification of Clay. USCS in the table means Unified Soil Classification System.

In Figure 2.8, the correlation of w_L and I_p is described by lower limit line (A-line) and the upper limit line (U-line). These lines are describe by equation 2.1 and 2.2. According to Casagrande (1932) who defined these lines, a result is consider as an error if its located over U-line while results located inside the limit lines indicates an exceptional plastic clay. Thus, base on the results of the four samples shown in Figure 2.8, all the samples used in this thesis are exceptional plastic clay and belongs to classification categories CS (super high plasticity clay) and CE (extremely high plasticity clay).

A-line:

$$I_p = 0.73(w_L - 20) \tag{2.1}$$

U-line:

$$I_p = 0.9(w_L - 8) \tag{2.2}$$

Where:

I_p	Plasticity index	[%]
w_L	liquid limit	[%]

Chapter 3

Soil Data

In this chapter, the soil data, test method, test programme , the results of the oedometer test and the measured swelling pressure are presented.

An oedoemeter test also known as consolidation test is widely use for the prediction of settlement of structures and swelling of soil. There are two methods of consolidation test, the constant rate strain CRS and incremental loading IL. Both methods gives a result showing strains vs stress however the difference is that CRS can often be completed faster than IL test. CRS test characterize the consolidation behavior of soil where the specimen is consolidated in a constant rate.

In this thesis, the tests was performed in 1-D IL eodometer test with double sided drain both in the upper and lower interface. This means that the consolidation rate is doubled compare to a single-sided drain. The consolidation test was conducted at Aalborg University using the GDS Automatic Oedometer System. The incremental loading oedometer test and constant volume method were performed based on DS (ISO/TS 17892-5).

3.1 Initial soil condition

Test	Depth [m]	Water content w [%]	Bulk density γ [kPa]	Void ratio e [-]	In-situ stress σ'_{v0} [kPa]
Test01	63	42.80	17.28	1.208	575
Test02	63	44.56	17.69	1.167	575
Test03	35	41.63	17.98	1.119	340
Test04	35	40.15	17.98	1.098	340

Table 3.1: Initial state parameters.

Table 3.1 presents the initial state parameters of the test samples. Four oedometer tests were conducted on Søvind Marl from Aarhus Harbour, namely, Test01, Test02, Test03 and Test04. Test01 and Test02 were tested in 24hr load step test. Test03 and Test04 were tested in 14day load step test. The samples of Test01 and Test02 were from the same tube in borehole LH900 (35 m depth) while the samples of Test03 and Test04 taken in same in the same tube from borehole LH830 (63 m depth).

3.2 Test Method

The test method of oedometer test is divided into two parts, the test preparation and test programme. Each part is decribed in the following procedures:

3.2.1 Test preparation

The oedometer parts used in test preparation are listed below which are shown in Figure 3.1.

Figure 3.1: Parts of Oedometer.(AAU lab).

1. Oedometer cell
2. Lower porous disk
3. Ring
4. Oedometer ring
5. Clamping ring
6. Lower porous disk
7. Pressure head
8. Screws

- First, the materials should be clean and dried and its mass and dimensions are measured. These materials are the upper pressure head m_u, upper pressure head including the filter m_{pu}, lower pressure head with the filter m_{pl} and oedometer ring m_r.
- The internal surface of the oedometer ring (4) is lubricated using a silicone spray. The dimensions of all oedometer rings used was 35 mm height and 35 mm diameter. This was used in order to reach the high stress level required in the test.
- The soil sample had been carefully extruded from the sampling tube into the oedometer ring using the extrusion device.
- The oedometer ring with sample inside was filled and levelled by trimming the excess soil, see Figure 3.2

Figure 3.2: The excess soil was trimmed and levelled. (AAU lab).

- The mass of the oedometer ring contained with levelled sample is measured. This is done in order to determine the mass of the sample where the oedometer ring with sample is subtracted to the mass of oedometer ring that was determined in the first procedure.

$$m_{pu} + m_{pl} + m_r + sample = m_{total} \tag{3.1}$$

$$sample = m_{total} - (m_{pu} + m_{pl} + m_r) \tag{3.2}$$

- The two porous plates is saturated by submerging in de-ionised water for about 20 minutes (DS (ISO/TS 17892-5) section 5.1.2.6). This is done in order that the porous plates are readily permeable to water.

- Assemble the oedometer cell by placing the parts from bottom to top. At the bottom, inside the oedometer cell (1), the lower porous disk (2) is place and a filter is place above on it in order to prevent intrusion of the soil. Place the oedometer ring (4) with the sample inside and put it inside the ring (3). At the top of the oedometer ring another porous disk (6) is place with a filter below on it.
- Place the loading ram at the top of the pressure head (7) on the top porous disk. The loading ram should be mounted centrally such that the load is axially applied. Place the clamping ring (5) and lock the cell body and secure it with screws provided (8).
- The two transducers are then installed and secured in position. These transducers are measuring the deformation of the specimen during the test.
- After assembling all the parts, the oedometer test can now be started. The final set-up of can be shown in Figure 3.3.

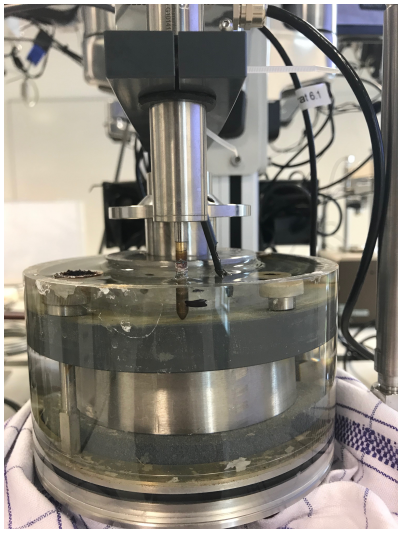

Figure 3.3: Installed oedometer cell filled with de-ionised water (AAU lab).

3.2.2 Test Programme

Swelling logging

- First, turn on the GDS Automatic Oedometer Apparatus. The soil description and the loading programme is set in the GDS keypad.
- The swelling logging is set first as the swelling pressure is evaluated in this thesis. When the swelling logging starts, submerge the specimen by pouring the de-ionised water into the oedometer cell. The de-ionised water should fully filled the whole

oedometer cell in order to make sure that sample has enough water for fully saturation. As constant volume method is performed in this thesis, the volume is constant (strain=0) and as swelling is prevented the pressure will generate instead. This pressure is the swelling pressure.

Oeodometer logging

- After the swelling logging was done then the oedometer logging according to loading programme starts. The loading programme used for all the tests with different duration is shown in Table 3.2. This will automatically performed in GDS oedometer apparatus according to the type of load step duration being used. The first load step should be higher on the measured swelling pressure from the previous so that the specimen will not swell again.
- After the tests, dismantle all the parts assembled. Take the mass of the oedometer ring with the compacted sample.
- Lastly, put the sample in the oven and determine the dry mass of the sample.

Test Plan			
Load Steps	σ' [kPa]	**24hr load step test** [day]	**14day load step test** [days]
Swelling logging	- -	1 -	approx. 4 months
1	300	1	14
2	600	1	14
3	1200	1	14
4	600	1	14
5	300	1	14
6	600	1	14
7	1200	1	14
8	2400	1	14
9	4800	1	14
10	2400	1	14
11	1200	1	14
12	2400	1	14
13	4800	1	14
14	10,000	1	14
15	300	1	14
		$\sum$ 16 days	$\sum$ 11 months

Table 3.2: Loading programme for short and long duration test in all 4 samples. Here the samples tested in 24hr load step tests took 16 days in total including the swelling logging phase. While in 14day load step tests, the tests were conducted in a period of 11 months (both in swelling logging and oedometer logging).

3.3 Test results

In this section, the result of the swelling logging and oedometer logging are presented.

3.3.1 Swelling logging result

Figure 3.4 shows the results of the measured swelling pressure in all 4 samples while the first 24 hours since the start of the test in Figure 3.4 are plotted as shown in Figure 3.5.

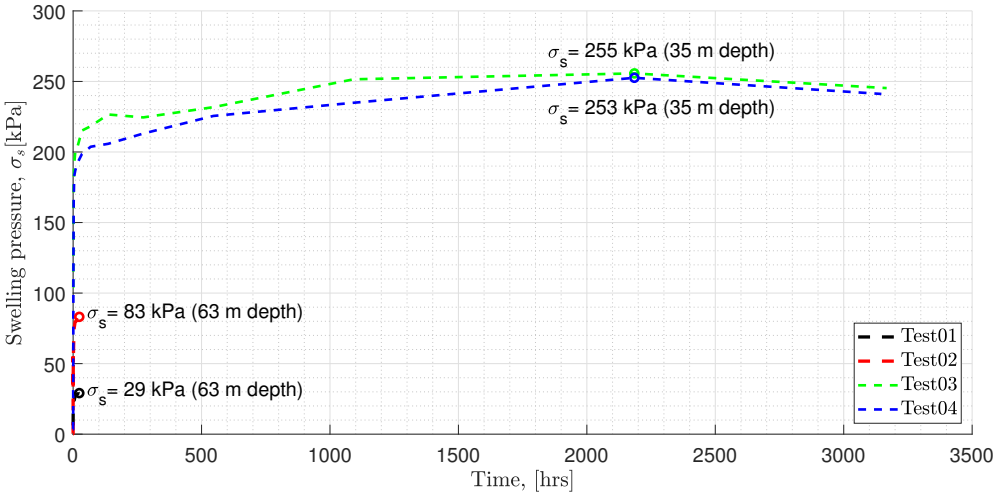

Figure 3.4: Measured swelling pressure for all the tests.

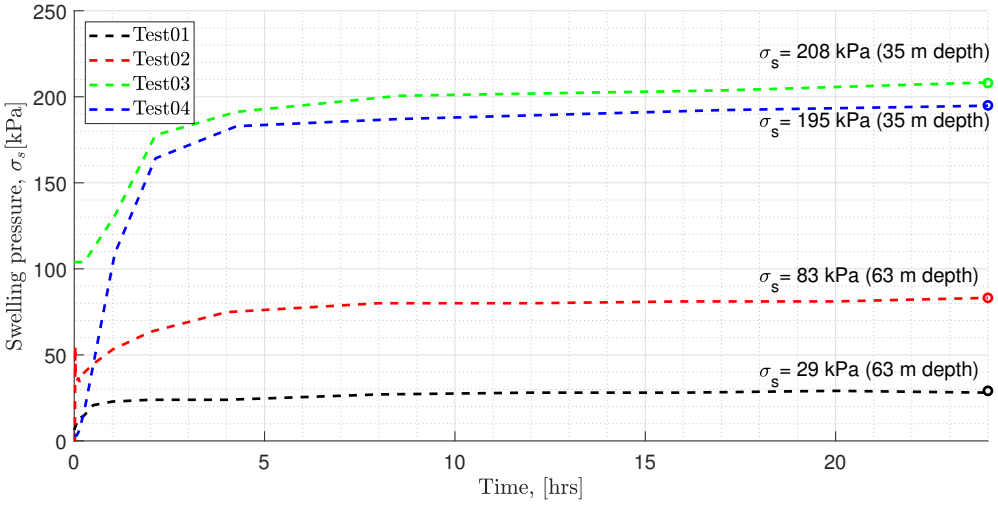

Figure 3.5: Measured swelling pressure after 24 hours in 4 samples.

The measured swelling pressure for the duration of 24 hour method have reached to 29 kPa and 83 kPa for Test01 and Test02, respectively. While the measured swelling pressure for Test03 and Test04 have reached to 255 kPa and 253 kPa for approximately three months. These results are discussed in Chapter 5.

3.3.2 Oedometer logging result

The data of the measured parameters during the oedometer test are shown in Table 3.3.

Parameter	Symbol	Measured unit
Initial height	H_0	[mm]
Initial diameter	D_0	[mm]
Initial mass	m_0	[g]
Stage number	$-$	[-]
Time since start of the test	t_t	[sec]
Time since start of the stage	t_s	[sec]
Stress target	σ_t	[kPa]
Displacement from the frame	δ_t	[mm]
Axial displacement 1	δ_1	[mm]
Pore pressure	u	[kPa]
Axial Load	P	[KN]
Axial displacement 2	δ_2	[mm]
Axial stress	σ	[kPa]
Axial strain1	ε	[%]

Table 3.3: Parameters measured during the oedometer test.

The outcome of the test programme can be plotted in terms of stress vs. strain or stress vs. void ratio. If the result is plotted in terms of strains, it is important to determine either the engineering strain or natural strain have to be use as there are significant difference between the two. The engineering strain ε^E is calculated according to equation 3.3 and the natural strain is calculated according to equation 3.4. The difference of the consolidation curve using the two types of strains are shown in Figure 3.6 for Test02.

$$\varepsilon^E = \frac{\delta}{H_0} \tag{3.3}$$

$$\varepsilon^N = \ln\left(\frac{H_0}{H_0 - \delta}\right) \tag{3.4}$$

Where:

H_0	Initial height	[mm]
δ	Displacement	[mm]

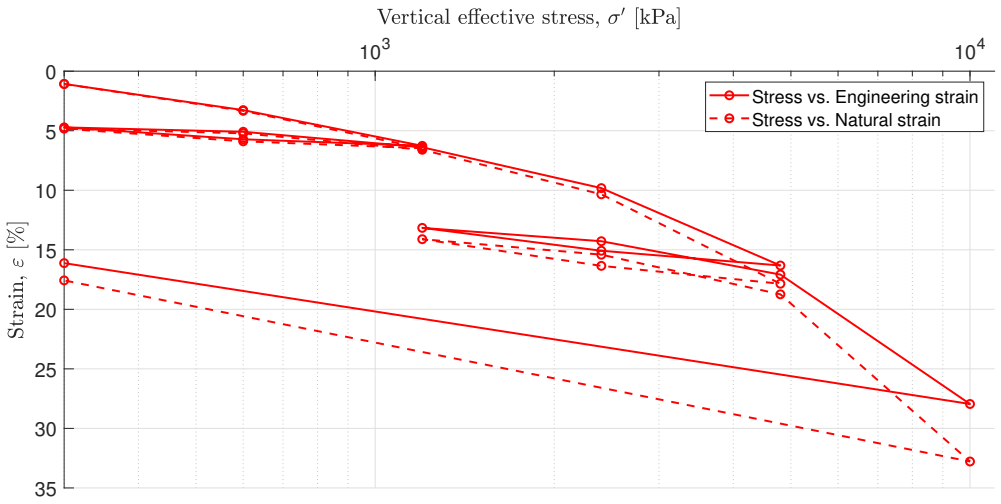

Figure 3.6: Difference between $log(\sigma) - \varepsilon^E$ curve and $log(\sigma) - \varepsilon^N$ curve in Test02.

In Figure 3.6, the difference of the consolidation is notable. At the lowest stress level, the $log(\sigma) - \varepsilon^E$ curve and $log(\sigma) - \varepsilon^N$ curve are almost similar, however, at the highest stress level the difference are very significant. This is evidently shown that the natural strain (true strain) gives a better description of the strains at highest stress level than the engineering strain and therefore used in further calculation. The outcome of the four tests performed in two different load duration steps plotted in terms of $log(\sigma) - \varepsilon^N$ curves are shown in Figure 3.7. The dashed curves are the result of the 24hr load step tests while the solid curves are the result of 14day load step tests. These curves will be analysed in the soil data analysis in Chapter 4. Moreover the interpretation of these curves are discussed in Chapter 5.

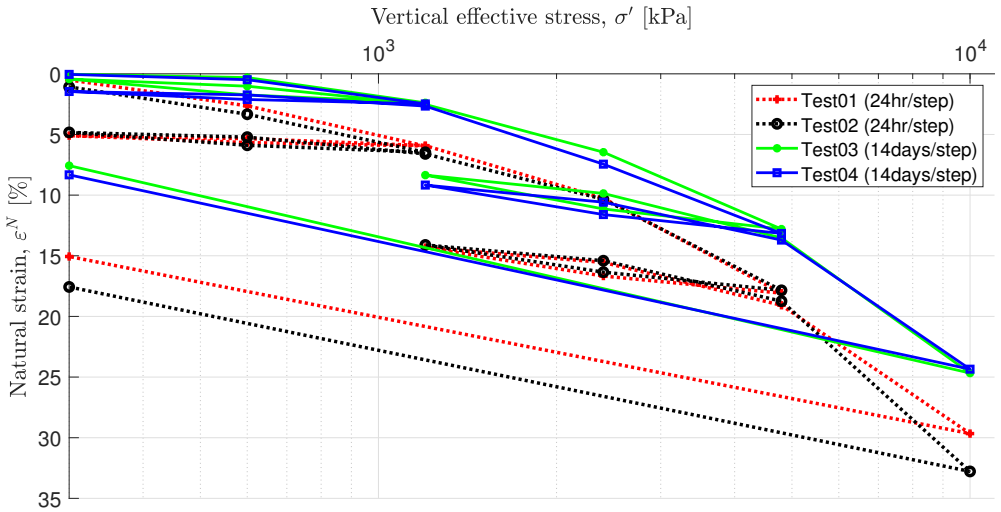

Figure 3.7: Consolidation curves of the four samples which will be use in data analysis

Chapter 4

Soil Data Analysis

This chapter covers the analysis of soil data. There are two stages of analysis presented in this chapter, namely, strain separation analysis and preconsolidation stress analysis.

The objective of strain separation analysis is to separate the consolidation strain and the creep strain. After the strains are separated, the consolidation strain is isolated and used further in the preconsolidation stress analysis. In this thesis, the Danish traditional methods, namely, Brinch Hansen and ANACONDA method are used. Furthermore, in preconsolidation stress analysis, σ_{pc} was determined using four methods, namely, Janbu, Akai, Pacheco Silva and Jacobsen method.

In this chapter, only Test04 in 14dayload step test is presented in order to illustrate specifically the whole process of data analysis. However, the results in other tests are summarised and presented in table at the end of each section. These results are discussed in Chapter 5. The overall results of the strain analysis showing the plots in each test and the outcome of the parameters obtained after the methods used are presented in Appendix C while the preconsolidation stress results can be found in Appendix D.

4.1 Strain separation analysis

In this section, the procedure in separating the strains using the two methods, Brinch Hansen and ANACONDA, are presented. These methods were applied each load step in all the tests. After the consolidation strain is isolated from the total strain, the consolidation strain in each load step are plotted against the effective stress σ'. After the continous stress-strain are constructed, the virgin compression index C_c is obtained.

4.1.1 Brinch Hansen method

The traditional method also called as $\sqrt{t} - \log(t)$ method was suggested by Brinch Hansen (1961). This method assumes that the creep strains starts after the consolidation strains ends. In addition, it also assumes that in $\sqrt{t} - \varepsilon$ graph, the consolidation strains is linear and the creep strains are also linear in $\log(t) - \varepsilon$ graph. The two graphs are then fitted at the beginning of $\sqrt{t} - \varepsilon$ and at the end of the data in $\log(t) - \varepsilon$ using a regression line as shown in Figure 4.1. In order to determine the consolidation and creep strains, these two graphs are combined, see Figure 4.1. The intersection of the regression line must intersect at measured time t equal to the time at which the consolidation ends t_c or T=1. Note that T is a dimensionless time factor which is calculated using equation 4.1. This is use to minimise the error of the intersection. Here an initial guess of t_c is updated until the two graphs in Figure 4.2 intersect at $T = 1$. This means that the intersection points is always happen at $T = 1$. Finally, the consolidation and creep strain are separated as shown in Figure 4.2.

$$T = \frac{t}{t_c} \tag{4.1}$$

where:

T	Dimensionless time factor [-]
t	Measured time [min]
t_c	End of consolidation time [min]

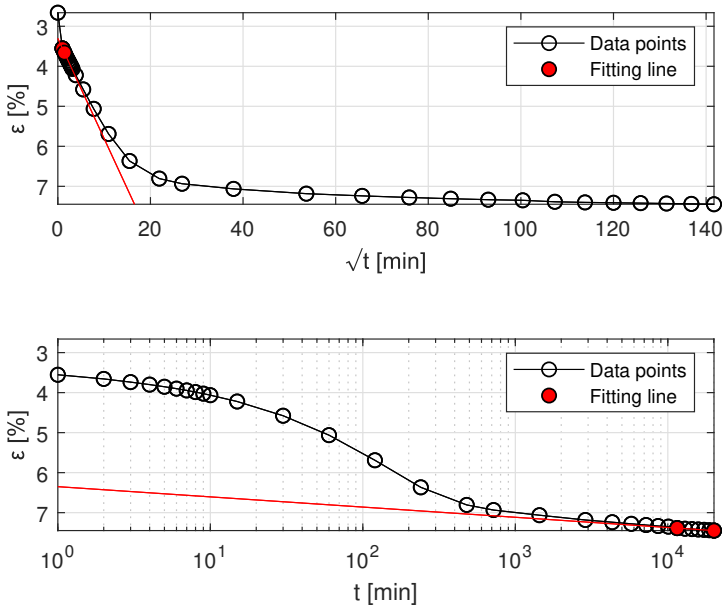

Figure 4.1: Determination of fitting lines in $\sqrt{t} - \varepsilon$ graph (top) and $\log(t) - \varepsilon$ (below) graph for step 8 Test04.

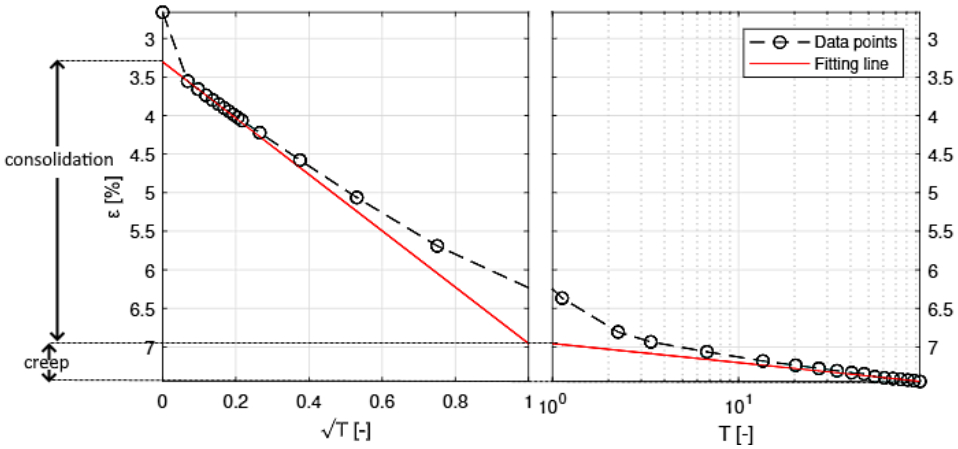

Figure 4.2: Consolidation and creep progress for load step 8 Test04 determined by Brinch Hansen's method. Here t_c is found to be 2326 min or 1.6 days.

4.1.2 ANACONDA Method

The **Ana**lysis of **Con**solidation test **Da**ta or ANACONDA method which is suggested by Bjerrum (1967) considers that the primary consolidation and the secondary consolidation process occurs simultaneously and independent to each other. A slightly overconsolidated clay was used and decribed by Bjerrums theory. The process in separating the consolidation and creep strains using ANACONDA method is described below.

1. Guessed the time t_A (the time before creep started) and add at the end of the tail slope of the total strains $(t_A + t_{end}; \varepsilon_{tot}^{end})$, see Figure 4.3. This inclination slope of $t_A + t_{end}; \varepsilon_{tot}^{end}$ is the secondary compression index $C_{\alpha\varepsilon}$.

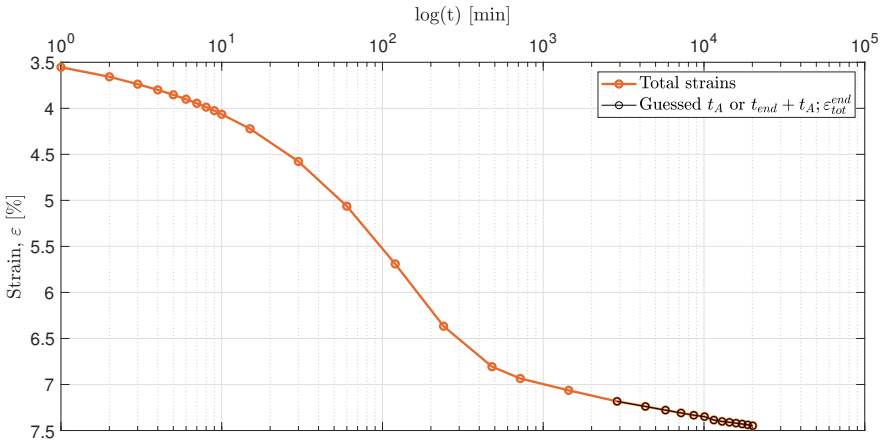

Figure 4.3: Guessed t_A that is added at the end tail of total strain curve for step 8 Test04. The inclination slope of $t_A + t_{end}; \varepsilon_{tot}^{end}$ is the secondary compression index $C_{\alpha\varepsilon}$.

2. Calculate $C_{\alpha\varepsilon}$ using equation 2.

$$C_{\alpha\varepsilon} = \text{slope of}(t_A + t_{end}; \varepsilon_{tot}^{end}) \tag{4.2}$$

3. Use the $C_{\alpha\varepsilon}$ slope to calculate the increase of creep strains $\Delta\varepsilon_{\alpha\varepsilon}$. An example is shown in Figure 4.4. The increase of $\Delta\varepsilon_{\alpha\varepsilon}$ is obtained using equation 4.3. Here time t is known from the load step and t_A is the guessed time.

$$\Delta\varepsilon_{\alpha\varepsilon} = C_{\alpha\varepsilon}\ log\left(1 + \frac{t}{t_A}\right) \tag{4.3}$$

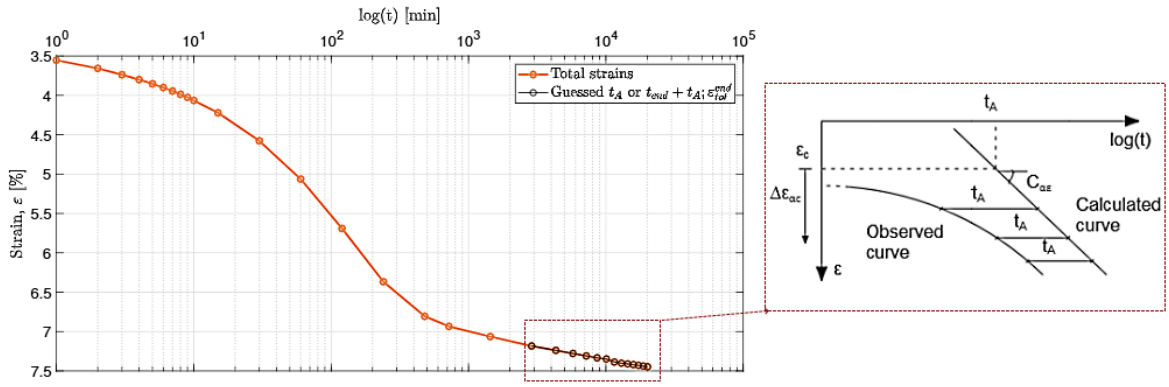

Figure 4.4: Calculate the increase of creep strains $\Delta\varepsilon_{\alpha\varepsilon}$ using equation 4.3. The highlighted data points inside the rectangle is zoom in to the right, shows an example on how to calculate $\Delta\varepsilon_{\alpha\varepsilon}$. The best guessed time t_A will transform $\Delta\varepsilon_{\alpha\varepsilon}$ into a straight line in semi-log plot when added to time t.

4. Calculate the consolidation strain using the $\Delta\varepsilon_{\alpha\varepsilon}$ found, given by equation 4.4, which should give a straight horizontal line at the tail of the consolidation strains curve (in blue), see Figure 4.5.

$$\varepsilon_c = \varepsilon_{tot}^{end} - \Delta\varepsilon_{\alpha\varepsilon} \tag{4.4}$$

5. If the tail of the consolidation strains curve (in blue) is equal to zero. Calculate the creep strain using equation 4.5. If the tail of the consolidation strains curve (in blue) is not equal to zero then back to step 1.

$$\varepsilon_{creep} = \Delta\varepsilon_{\alpha\varepsilon} + \varepsilon_c \tag{4.5}$$

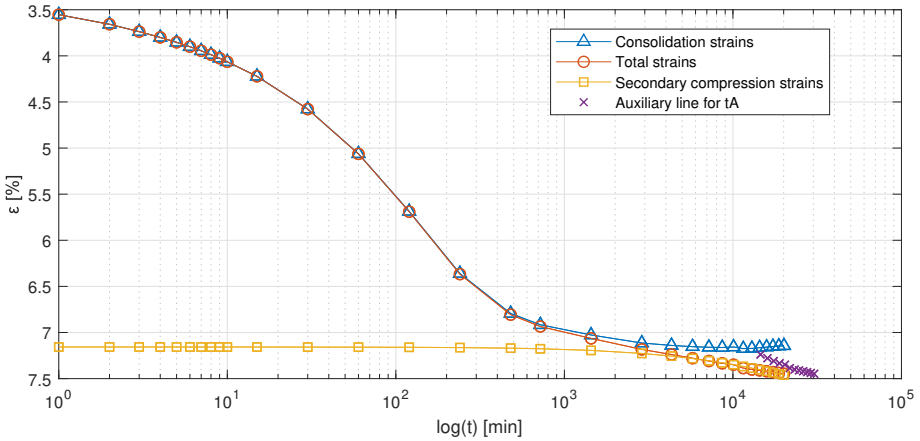

Figure 4.5: ANACONDA method used on load step 8 Test04. The curves (in blue) is the consolidation strains, total strains (in orange), creep strains (in yellow) and the auxiliary line for $t_A + t_{end}; \varepsilon_{tot}^{end}$ (in purple).

4.2 Compression Index

The slope of the compression index C_c can be determined after the outcome of the strain separation analysis. Figure 4.6 shows the result of the strain separation analysis in Test04.

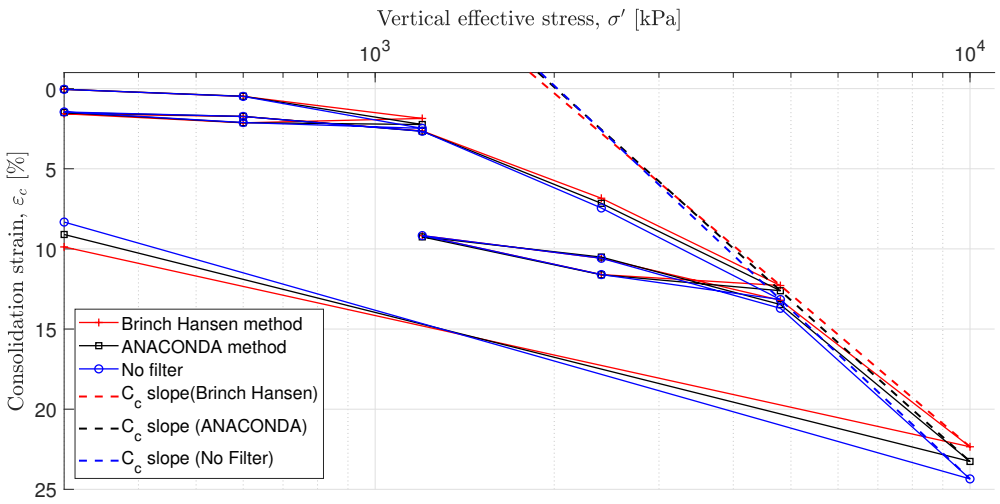

Figure 4.6: Virgin compression index C_c in Test04. No filter curve is the $log(\sigma) - \varepsilon^N$ curve where no strain separation is applied.

The compression index is determined using equation (4.6). The overall results are presented in Table 4.1 for all the tests.

$$C_c = \frac{\Delta\varepsilon_c}{\Delta \log(\sigma')} \tag{4.6}$$

where:

$\Delta\varepsilon_c$	Increase in consolidation strains along the compression curve [%]
$\Delta \log(\sigma')$	Increase in $\log(\sigma')$ along the compression curve [%]

Method	Test01 C_c [%]	Test02 C_c [%]	Test03 C_c [%]	Test04 C_c [%]
Brinch Hansen	32.29	35.29	36.04	31.55
ANACONDA	35.24	42.32	34.91	33.41
No Filter	36.31	46.85	34.53	35.10

Table 4.1: Determined compression index C_c.

4.3 Preconsolidation Stress

This section presents the calculation of preconsolidation stress σ'_{pc} after the strain separation analysis is done. The methods used for the calculation of σ'_{pc} were Janbu, Akai, Pacheco Silva and Jacobsen method.

Preconsolidation stress $\sigma_{pc'}$ is the maximum stress that the soil has sustained in the past, e.g. glacial period. This geotechnical parameter is very important to engineers to determine before any construction in order determine the expected settlement of the foundations and the amount of load can be exerted on a soil without producing a large deformation. When the existing effective stress in the soil is equal to the maximum stress in the past (σ'_{pc}), the soil is called normally consolidated NC soil. If the existing effective stress in the soil is less than the maximum stress in the past, the soil is considered to be overconsolidated OC soil (preconsolidated). These type of soil are categorised based on the overconsolidated ratio OCR, which is defined in equation 4.3. The soil deformation (settlement) is larger in NC soils than OC soils.

$$OCR = \frac{\sigma'_{pc}}{\sigma'} \tag{4.7}$$

where:

$OCR = 1$	Normally consolidated soil
$OCR > 1$	Overconsolidated soil

4.3.1 Akai method

The determination of σ'_{pc} in this method is based on the secondary compression index $C_{\alpha\varepsilon}$ and effective stress σ'. $C_{\alpha\varepsilon}$ is the linear portion of the secondary compression in $\log(t) - \varepsilon_c$ curve and is calculated using equation 4.8. Akai (1960) found that $C_{\alpha\varepsilon}$ increases linearly when σ' is less than σ'_{pc}. When the σ' is greater than σ'_{pc}, the σ' increases in a logarithmic scale. When the curve breaks, an interval of σ'_{pc} (minimum and maximum σ'_{pc}) are determined. This is shown in Figure 4.7 for Test04 after the strain is separated by ANACONDA and Brinch Hansen's method. The determined σ'_{pc} for all the tests after using Akai's method are shown in Table 4.2.

$$C_{\alpha\varepsilon} = \frac{\Delta\varepsilon_c}{\Delta\log(t)} \tag{4.8}$$

where:

$\Delta\varepsilon_c$	Increase in consolidation strain during the secondary compression process	[-]
$\Delta\log(t)$	Increase in $\log(t)$ corresponding to $\Delta\varepsilon_c$	[-]

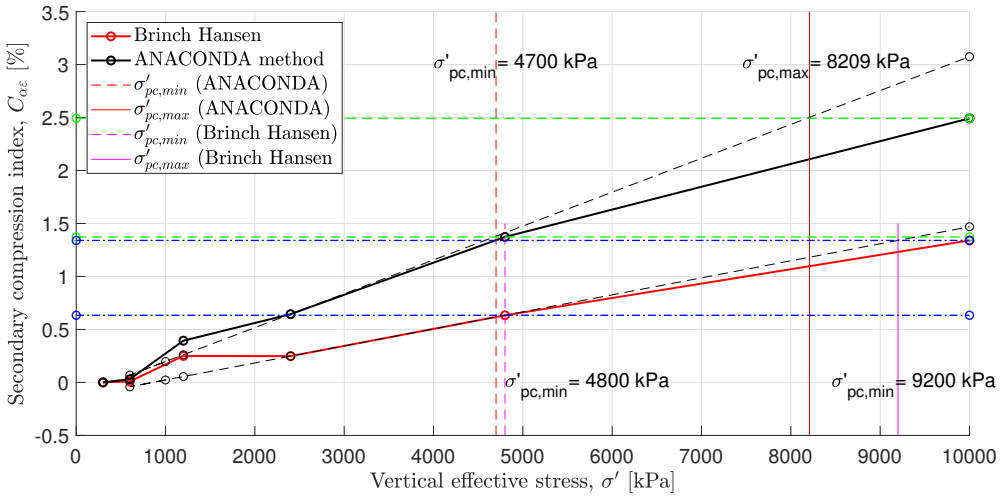

Figure 4.7: Akai method used in Test04 after the strain is separated by ANACONDA (black) and Brinch Hansen's method (red). Here the vertical lines are the minimum (dashed vertical lines) and maximum (solid vertical lines) σ'_{pc} found.

Method	Test01		Test02		Test03		Test04	
	$\sigma'_{pc,min}$ [kPa]	$\sigma'_{pc,max}$ [kPa]	$\sigma'_{pc,min}$ [kPa]	$\sigma'_{pc,max}$ [kPa]	$\sigma'_{pc,min}$ [kPa]	$\sigma'_{pc,max}$ [kPa]	$\sigma'_{pc,min}$ [kPa]	$\sigma'_{pc,max}$ [kPa]
Brinch Hansen	4800	6300	4800	8450	5190	8505	4800	9200
ANACONDA	4800	6100	4800	9500	4939	7465	4700	8209

Table 4.2: Determined σ'_{pc} based on Akai's method.

4.3.2 Janbu method

Janbu (1969) method determine the σ'_{pc} based on consolidation modulus, M, plotted against the effective mean stress, σ'_m. The consolidation modulus M is determined given in equation (4.9) and σ'_m is the average of the previous and current stress applied. σ'_{pc} is determine when there is a drastic change in $\sigma'_m - M$ curve and this is happened when M exceeded σ'_{pc} level. When σ'_{pc} is reached, M decreases and tends to follow the the m slope defined by the compression index C_c defined in equation 4.10.

$$M = \frac{\Delta\sigma'}{\Delta\varepsilon_c} \tag{4.9}$$

Where:

$\Delta\sigma'$	Effective stress difference in previous and current stress applied	[kPa]
$\Delta\varepsilon_c$	Consolidation strain difference in previous and current strain applied	[%]

$$m = \frac{\log(10)}{C_c}\sigma'_m \tag{4.10}$$

where:

C_c	Compression index	[-]
σ'_m	mean of previous and current stress	[kPa]

Figure 4.8 shows the $\sigma'_m - M$ plot in Test04. Here at low σ'_m level the M has the highest value. This means that the deformation produced is small. As σ'_m increases, M suddenly drops. According to Janbu (1969), σ'_{pc} is obtained where the intersection of the slope of the descending part of the curve and the line of the minimum value of M. After σ'_{pc} is determined, M starts to increase and follows the m slope.

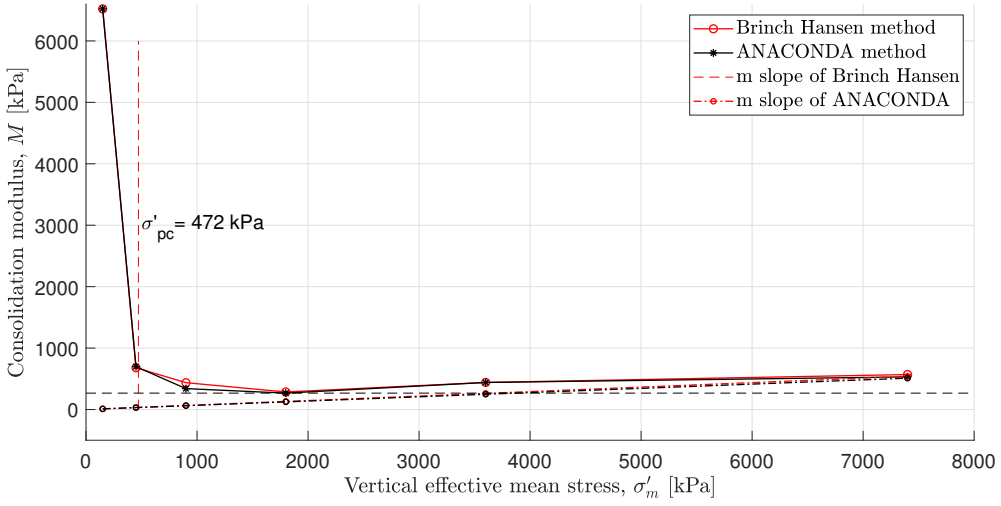

Figure 4.8: Janbu method used in Test04 after the strain is separated by ANACONDA and Brinch Hansen method.

The determined σ'_{pc} for all the tests after using Janbu's method are shown in Table 4.3.

Method	Test01 σ'_{pc} [kPa]	Test02 σ'_{pc} [kPa]	Test03 σ'_{pc} [kPa]	Test04 σ'_{pc} [kPa]
Brinch Hansen	450	450	483	472
ANACONDA	450	450	483	472

Table 4.3: Determined σ'_{pc} based on Janbu's method..

4.3.3 Pacheco Silva method

Pacheco Silva (1970) method determines σ'_{pc} using an empirical construction in $log(\sigma') - \varepsilon_c$ curve. Here a horizontal line is constructed at the initial strain ε_0 and the virgin curve is straightly extented upward until the two lines intersect. At the intersection point (A), a vertical line is drawn downward until it reaches the $log(\sigma) - \varepsilon_c$ curve at point (B). From that point, draw a horizontal line towards the virgin curve until it will intersect. This intersection point gives the value of σ'_{pc} which can be shown in Figure 4.9 for Test04 where the strains are separated using ANACONDA method and Brinch Hansen's method.

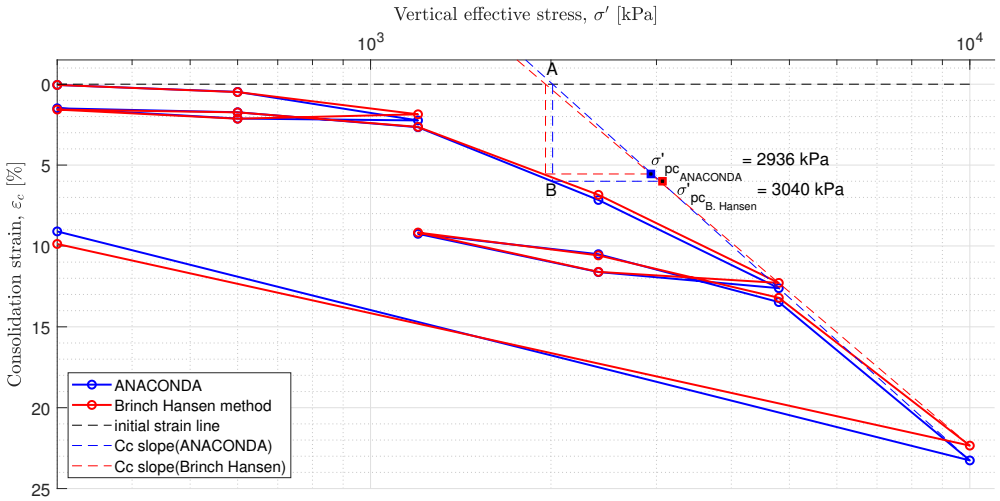

Figure 4.9: Pacheco Silva method used in Test04 after the strain is separated by ANACONDA and Brinch Hansen method.

The determined σ'_{pc} for all the tests are presented in Table 4.4.

Method	Test01 σ'_{pc} [kPa]	Test02 σ'_{pc} [kPa]	Test03 σ'_{pc} [kPa]	Test04 σ'_{pc} [kPa]
Brinch Hansen	2676	3087	2985	2936
ANACONDA	2508	3053	3088	3040

Table 4.4: Determined σ'_{pc} based on Pacheco Silva method.

4.3.4 Jacobsen method

Jacobsen (1992) method is a combination of Terzaghi's theory and the construction of Casagrante to determine the σ'_{pc}. The principle of Jacobsen's method is to determine σ'_k which is the stress level added to σ', that gives the virgin compression line linear in logarithmic graph as shown in Figure 4.10. In the figure, the first points of the data curve are ignored in the fitting. According to Jacobsen (1992) these points can lead to a high values of σ'_k in the fitting optimization. Hereby, σ'_{pc} can be estimated using equation (4.11). The determined values for all the tests are shown in Table 4.5.

$$\sigma'_{pc} = 2\,\sigma'_k \tag{4.11}$$

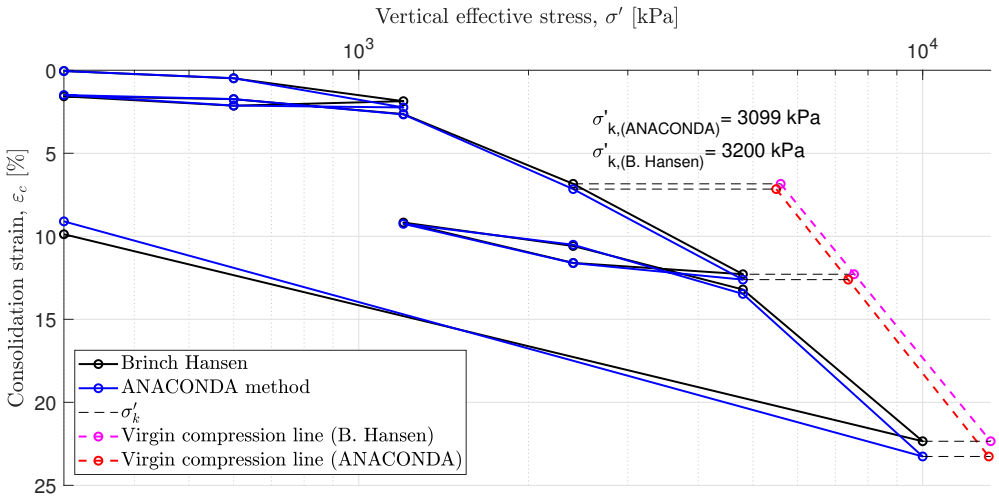

Figure 4.10: Jacobsen method used in Test04 after the strain is separated by ANACONDA and Brinch Hansen method.

Method	Test01 σ'_{pc} [kPa]	Test02 σ'_{pc} [kPa]	Test03 σ'_{pc} [kPa]	Test04 σ'_{pc} [kPa]
Brinch Hansen	4314	5168	6485	6198
ANACONDA	4317	5510	6740	6400

Table 4.5: Determined σ'_{pc} based on Jacobsen method.

4.4 Results

In this section, the outcome of strain separation analysis on Test01, Test02, Test03 and Test04 are shown in the figures below. Additionally, the determined preconsolidation stress using Janbu, Akai, Pacheco Silva and Jacobsen's method are summarised in Table 4.6. The parameters obtained by the strain separation methods are presented in tables in Appendix C and the plots in all the tests using different methods in the determination of preconsolidation stress can be shown in Appendix D. The interpretation and discussion of these results are discussed in Chapter 5.

Strain separation results

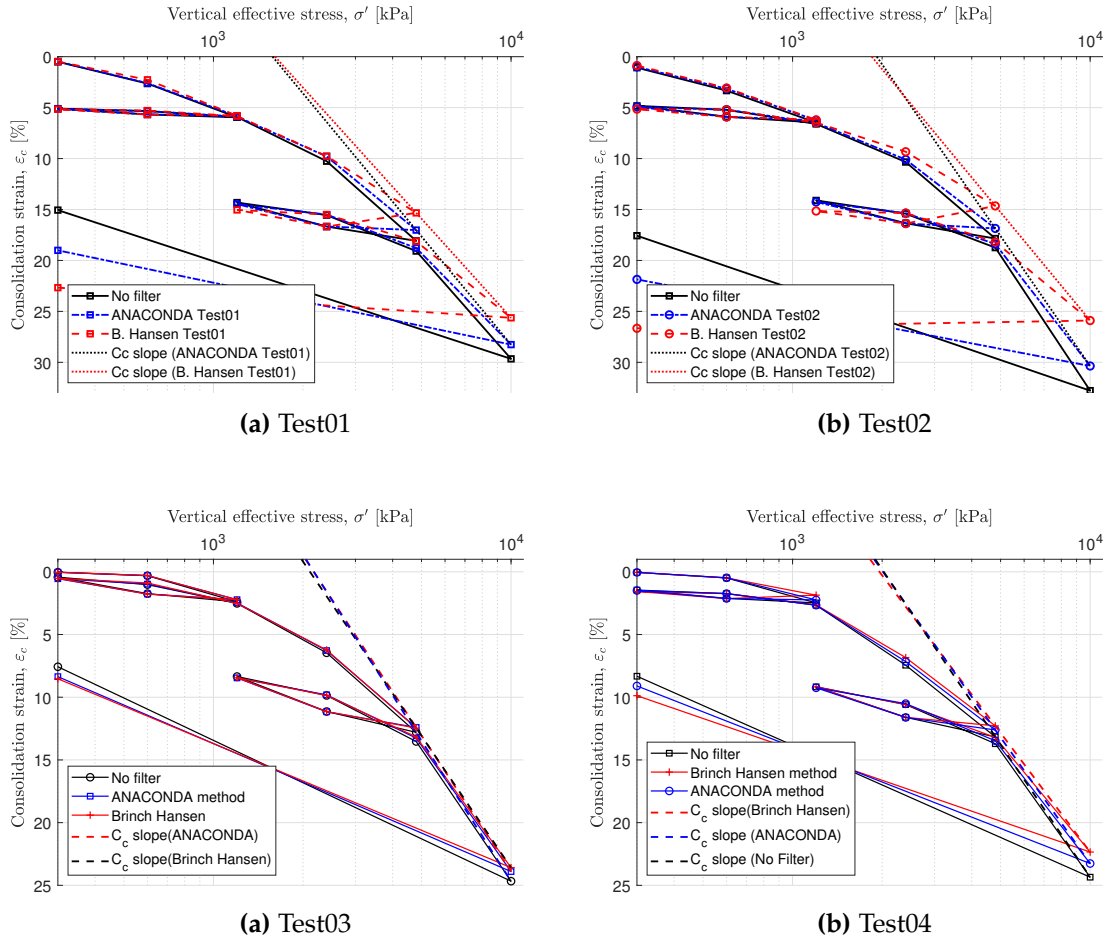

(a) Test01 **(b)** Test02

(a) Test03 **(b)** Test04

Figure 4.12: Strain separation analysis results in all the tests. Test01 (a) and Test02 (b) are the 24hr load step tests. Test03 (c) and Test04 (d) are the 14day load step tests. No filter curve (black) is the $log(\sigma) - \varepsilon^N$ curve where no strain separation is applied.

Preconsolidation stress results

Methods	Test01 (24hr/load-step)		Test02 (24hr/load-step)		Test03 (14days/load-step)		Test04 (14days/load-step)	
	ANACONDA [kPa]	B. Hansen [kPa]	ANACONDA [kPa]	B. Hansen [kPa]	ANACONDA [kPa]	B. Hansen [kPa]	ANACONDA [kPa]	B. Hansen [kPa]
Janbu	450	450	450	450	483	483	472	472
Pacheco Silva	2508	2676	3053	3087	3088	2985	3240	2936
Jacobsen	4317	4314	5510	5168	6740	6485	6198	6400
Akai	4800-6100	4800-6300	4800-9500	4800-8450	4939-7465	5190-85056	4700-8209	4800-9200

Table 4.6: Preconsolidation stress results.

Chapter 5

Interpretation and Discussion

This chapter focus on the interpretation and discussion of the results from the data analysis described in Chapter 4. This chapter consists of three sections where the interpretation and discussion on swelling pressure results, strain separation results and preconsolidation stress results are presented. In addition, a correlation analysis was made to get a better comparison of the consolidation parameter results obtained from different methods.

5.1 Swelling pressure results

5.1.1 Introduction

Table 5.1 presents the plasticity index and calcite content of the test samples in two different depths. The plasticity index was determined using fall-cone method on the soil samples used in this thesis (see section 2.3) while the calcite content was based on the experiments made by Grønbech (2014) in the same borings used in this thesis.

Tests	Depth [m]	Plasticity index [%]	Calcite [%]
Test01	63	157.7	8-10
Test02	63	150.8	8-10
Test03	35	111.6	36-38
Test04	35	108.4	36-38

Table 5.1: The plasticity and calcite content of all soil samples. The calcite content was based on the experiments results made by Grønbech (2014) in the same borings used in this thesis.

It can be seen that the soil samples at 63 m depth has higher plasticity than in the upper depth. This is due to the smectite mineral presents at 63 m depth which is believed to be higher on this depth. The higher the smectite content in the clay, the more expansive (more plastic) the soil will be. Additionally, based on the experiments made by Grønbech (2014), it was found that calcite content is higher at 35 m than in the lower depth. As shown in Table 5.1, the calcite and plasticity index on this clay are inversely correlated. An increasing calcite content present in Søvind Marl reduces the level of clay's plasticity.

In general, calcite is often used in the construction industry to stabilise the soil, reduce the plasticity index and swelling potential of the soil. Calcite is well known as a good flocculators of soil. When this mineral is present in the clay, the layers of clay particles will flocculate that will increase the permeability of the clay causing the water to drain out easily. This can be seen in Figure 5.1 (a) where the spacing of the particles is large (the permeability is high). For a dispersed structure, such as shown in Figure 5.1 (b) shows an oriented arrangement of clay particles. Clays that are highly overconsolidated (as in the case of Søvind Marl) due to the load subjected by glacial or volcanic acitvity would tend to be more dispersed structure. It can be seen that the spacing between clay particles in flocculated structure is larger than in a dispersed structure. It is evident that swelling on clay is less effective in flocculated structure than in a dispersed structure.

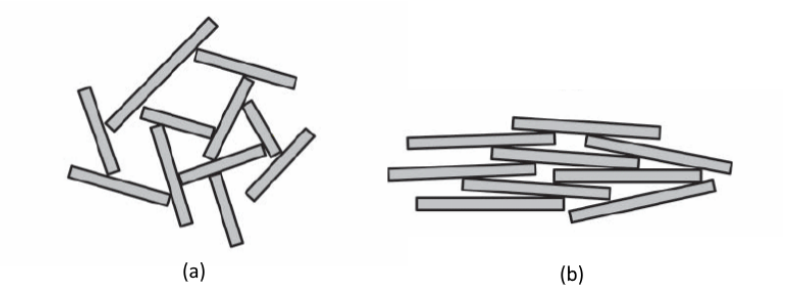

Figure 5.1: Clay particle associations. (a) flocculated structure which shows an edge-to-edge or edge-to-face association of clay particles (b) dispersed structure which shows an orriented arrangement of clay particles. When calcite is present in the clay, the layers of clay particles will flocculate (flocculated structure) that will increase the permeability of the clay causing the water to drain out easily. Thus, swelling on clay is less effective in flocculated structure than in a dispersed structure. John D. Nelson (2015)

5.1.2 Interpretation of swelling pressure results

The results on the swelling pressure in four samples in two different depths are shown in Figure 5.2(a). The swelling pressure measured 24 hours after the start of the tests in Test03 and Test04 from Figure 5.2(a) are then plotted in Figure 5.2(b) in order to see the difference clearly.

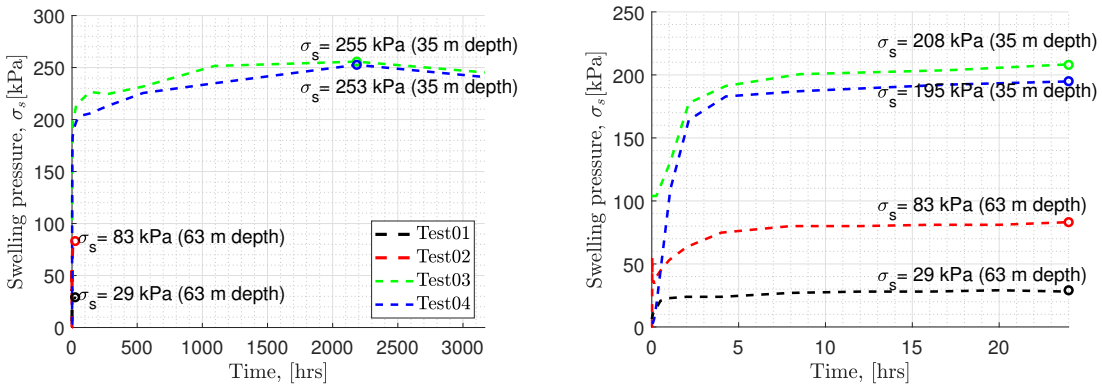

(a) **(b)**

Figure 5.2: (a) Measured swelling pressure results in all the tests samples. (b) Results in Figure 5.2(a) 24 hours after the start of the test.

Based on the discussion in previous section, the samples from 35 m depth is believed to be more flocculated due to the higher level of calcite present and expected to swell less. However, the swelling pressure results at 35 m depth samples are higher than the swelling pressure results at 63 m, see the figures in Figures 5.2. The swelling pressure are 3 to 8 times smaller in 63 m than in the upper depth (35 m). The reason could be that these samples had lost their potential to swell due to soil disturbance or the quality of the samples. However, the purpose of this test is to investigate the effect of load duration (short and long duration) on swelling pressure. This can be done by extracting the measured swelling pressure 24 hours after the start of the test in the soil samples from 35 m, see Figure 5.3(a) and compare on the swelling pressure measured after three months shown in Figure 5.3(b).

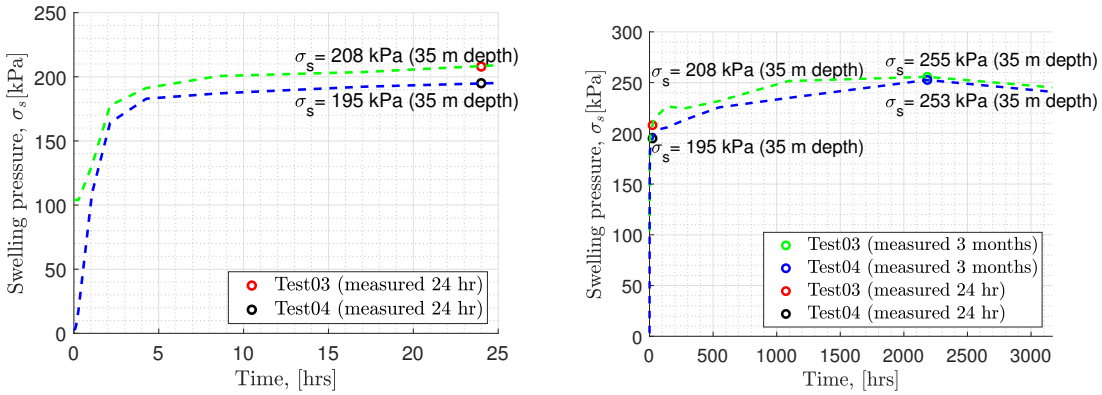

(a) **(b)**

Figure 5.3: (a) Measured swelling pressure 24 hours after the start of the test in the soil samples from 35 m. (b) Measured swelling pressure results in after 24 hours and three months.

In Figure 5.3(a), it is evident that within 24 hours the swelling pressure is still developing. This means that the clay is still exerting the pressure and the clay is still attempting to swell. The clay was completely arrested (i.e. not allowed to swell) after 3 months of test. There is one particularity to notice in Figure 5.3(a) on how fast the Søvind Marl reacted when wetted. The swell pressure grows rapidly for less than two hours after saturation. This is due to the water that was absorbed by smectite minerals.

The interaction of water on smectite clay particles consists of two phases. The first phase is the crystalline swelling which is the adsorption of water molecules occurs at inter-layer spacing. The second phase is the osmotic swelling, here the concentration of water molecules between the clay particles causes the water to be drawn into the inter-particle spacing due to osmotic pressure (John D. Nelson (2015)). The swelling is spontaneous if the salinity of the water used in saturation is not the same as the salinity of the pore water in the specimen.

In this thesis, de-ionised water was used for soaking the specimen. As Søvind Marl is a marine deposit, meaning the pore water is saline, the measured swelling pressure result has an additional swelling caused by osmotic pressure. According to Thøgersen (2001), the water composition will less influence the results if the test water resembles the natural pore water of the soil sample. The chloride concentration and pH (potential hydrogen) value of the pore water of the clay should have determined for mixing the correct salinity of the water used in saturation as this could lead to inaccurately determined the precise swelling pressure. It would be more correct to use that water, but this was not known at the time of the experiment. However, the point here is to investigate the effect of letting the sample to fully swell until the stress is determined that can resist the swell pressure in the specimen during the testing compared to the traditional 24 hour measurements.

5.2 Interpretation on the stress-strain curve results

Four oedometer tests were performed to investigate the effect of letting the Søvind Marl to fully consolidate during the tests and compared to the traditional 24 hr measurements. The stress-strain curve results are shown in Figure 5.4. All the curves show similar trends.

At the beginning of this study, the expectation was to get higher values of strains in long duration test (14day load step tests) than in the short duration test (24hr measurements) as the soil samples were consolidated in a longer duration of time. However, as shown in Figure 5.4, instead the curves of 24 hour measurements (Test01 and Test02) are greater than the curves of the samples tested in a long duration tests (Test03 and Test04).

All soil samples were at zero deformation prior to the start of oedemeter logging. However, 1 min after the application of the first load (300 kPa), there was evidence of considerable differences in the consolidation characteristics of the two soil samples, see Figure 5.5(a).

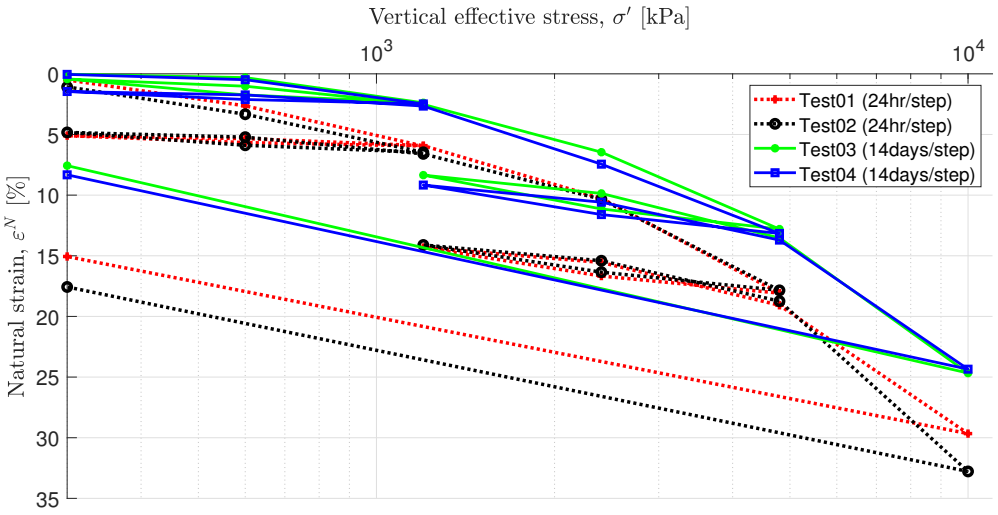

Figure 5.4: Stress vs. natural strain curves results in all tests.

Here the samples used in Test03 and Test04 (from the same boring at 35 m depth) were very stiff as the soil is not responding to the load in contrast to the consolidation characteristics of the samples in Test01 and most specifically in Test02.

In step 2 with a load of 600 kPa, the soil samples in Test03 and Test04 were slowly deformed but still have a major difference compared to Test01 and Test02, see Figure 5.5(b). In step 2 Test03, the test was manually skipped by accident and had measured only for 24 hours. However this error has less influence on the measurement of the final strain (in this step) as the deformation is almost constant. From step 3 to 15, the the structures of strain-time curves in two different duration tests shows similar behavior, these steps are presented in Appendix B.

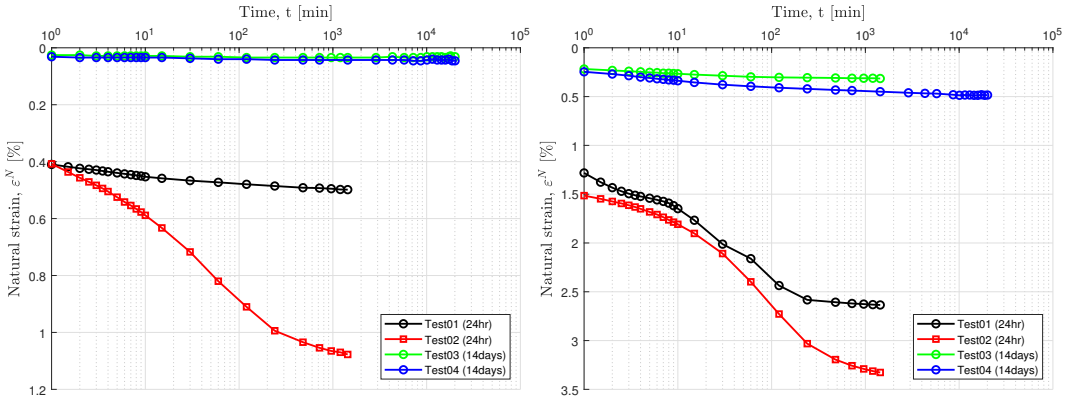

(a) Step 1 with a constant load of 300kPa. **(b)** Step 2 with a constant load of 600kPa.

Figure 5.5: Time vs. total strain in load step 1 and step 2.

The variations of time vs. natural strain curves in two samples used in two different duration tests were due to the fissures on Søvind Marl. Fissures substantially influence the stiffness of the clay at lower stresses Grønbech (2015). As the stress increases, the fissures will be forced to close leading to a gradual drop of the consolidation modulus M (stiffness of the clay). This is evidently shown in Figure 5.6. The fissures were already closed on the soil samples in Test01 and Test02 at a vertical mean effective stress σ'_m of 450 kPa while in Test03 and Test04, the fissures were completely closed after a σ'_m of 900 kPa. When the fissures are closed, the stiffness of the intact clay begins to dictate the behavior of the sample. As shown in the figure, the stiffness of the samples are almost identical as the σ'_m increases to 7400 kPa.

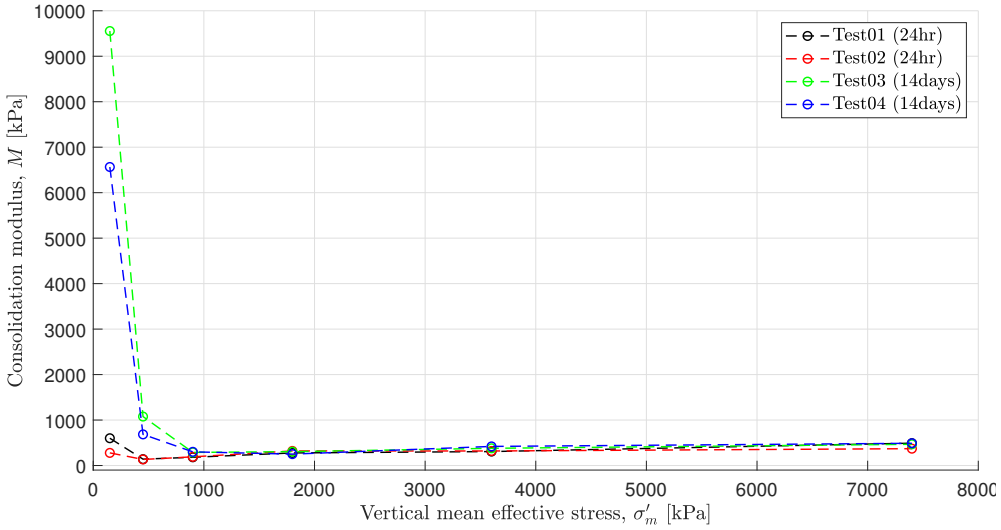

Figure 5.6: σ'_m vs. M graph. A gradual drop of the consolidation modulus M at lower stress level was due to the closure of fissures. Here consolidation modulus in Test01 and Test02 is less than Test03 and Test04.

In addition, Bishop (1965) and Skempton (1969) determined that the fissured structure has a large influence on the stiffness of the clay and both found that the spacing between fissures widens with depths. If the spacing between the fissures widens the stiffness will decrease as the clay structures are not intact. In this thesis, the samples used in Test01 and Test02 were from the same boring from 63 m while the samples used in Test03 and Test04 were from the same boring from 35m. Hence, the consolidation modulus in Test01 and Test02 is less than Test03 and Test04 as shown in Figure 5.6

As the loading sequences continued and the time vs. strain curves for each load step were plotted, the significant difference in the deformation from the first load step became even more apparent as the data compilations progressed. This is the reason why the final maximum strain in 24 hr measurements is greater than the 14day load step tests.

5.3 Discussion on the separation of strains results

ANACONDA method results

As explained in the iteration process of ANACONDA method in Chapter 4, the user has to guess the time before the creep has started in order to obtain the consolidation strain. It is a trial and error process until the tail slope of the consolidation strains will be equal to zero.

The interpretation of the result of ANACONDA method depends on the user experience and judgement. This method will be valid if the constant creep strain can be subtracted from the total strains and get a horizontal line in the log(time)-strain plot. Another way is to analyse the log(time)-strain curve where the ANACONDA method is only valid if the deformation curve ends in a log-linear line (the sign that primary consolidation has been completed). An example is shown in Figure 5.7 on step 14 Test03 (14day load step test). Here the consolidation strains found completed at approximately 2 days.

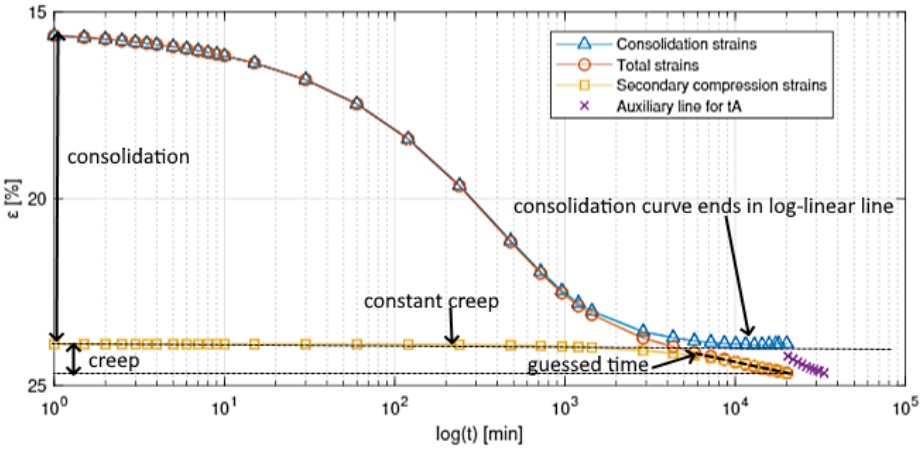

Figure 5.7: Outcome of Test03 step 14 which shows a valid strain separation using ANACONDA as consolidation curve ends in log-linear line is clearly shown. Here the consolidation strains found completed at approximately 2 days.

Figure 5.8 shows the outcome of ANACONDA when the consolidation and creep strains are separated in 24hr measurements for step 14 Test01. It can be seen that the performance of ANACONDA is not as definite as what is illustrated in Figure 5.7. Here the consolidation was already completed at approximately 7.5 hours. This is 40.5 hours in difference compared to Test03. In addition, it is noticeably shown that the consolidation end curve (in blue) in Test01 (step 14) is not completely linear compared to the consolidation end curve in Figure 5.7.

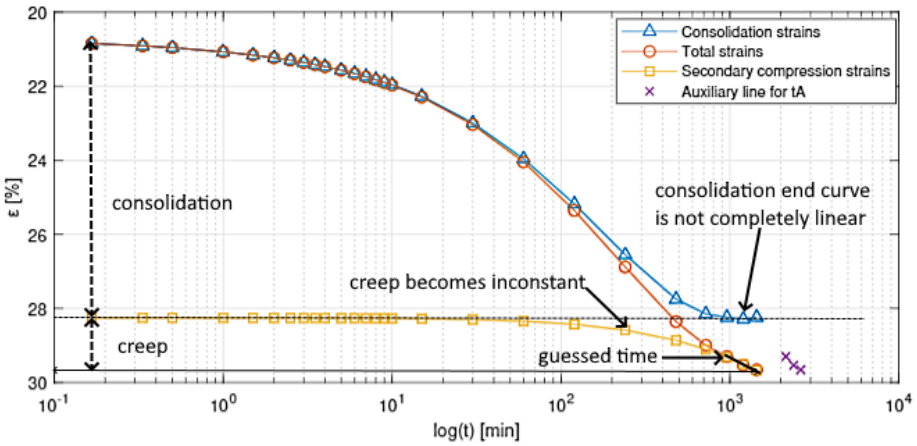

Figure 5.8: The outcome of Test01 step 14. The tail slope of the consolidation strains is not totally horizontal. Here the consolidation strains had reached at approximately 7.5 hours.

Brinch Hansen method results

As explained in Chapter 4, to determine the consolidation and creep strains, the two graphs of $\sqrt{t} - \varepsilon_c$ and $\log(t) - \varepsilon_c$ are combined, see Figure 5.9(a) and Figure 5.10(a) for Test03 and Test01 respectively. The intersection of the regression line must intersect at the measured time t equal to the time at the end of consolidation t_c. The outcome of Test03 (14 days) step 14 is shown in Figure 5.9(b) while the outcome of Test01 (24 hr) step 14 is shown in Figure 5.10(b). For load step 14 in Test03 (14 days), the end of consolidation found to be t_c = 2497 hrs (1.7 days) while for load step 14 in Test01 (24 hr) t_c = 2.26 hrs.

However, there are some issues on the consolidation curve performed in a 24hr load step tests. When the incremental load increases from 4.8 to 10 MPa (which makes the creep component to increase as well), resulting a steep slope particularly in $\log(t) - \varepsilon_c$ graph as shown in Figure 5.10(a) (left). The slope of the secondary compression index $C_{\alpha\varepsilon}$ ends up being high (which gives high creep strains), see Figure 5.10(b). According to Brinch Hansen (1961), one of the presumption of the developed model is that the creep consolidation proceed after many years according to the logarithmic law (a sign that the end curve in $\log(t) - \varepsilon_c$ ends in a horizontal tail). A proper example is shown in Figure 5.9(a). However, this presumption is disregarded in Figure 5.10(a) (left) for the 24 hour measurement due to the said slope.

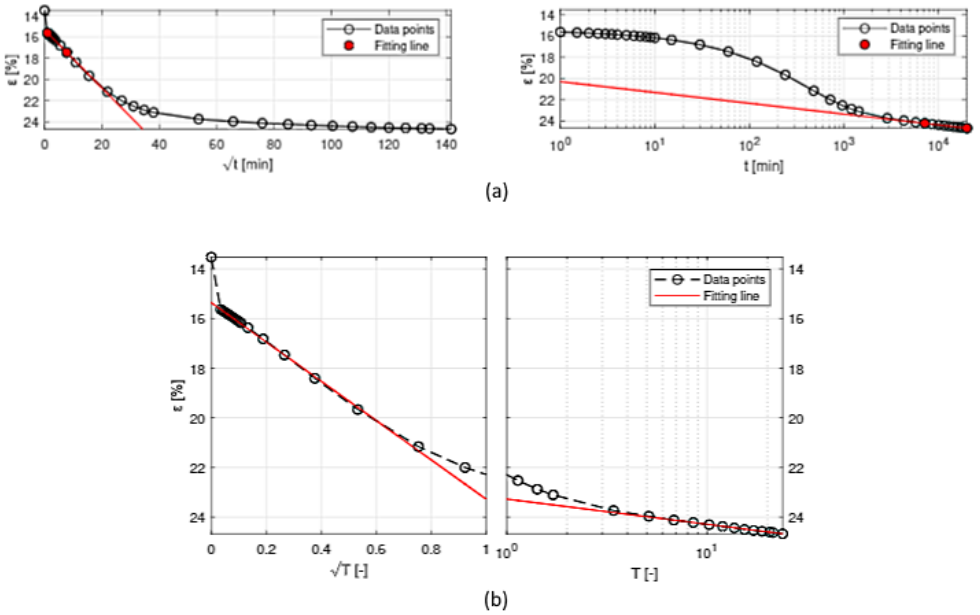

Figure 5.9: (a) Determination of two regression lines in $\sqrt{t} - \varepsilon_c$ and $\log(t) - \varepsilon_c$ in Test03 step 14. (b) The intersection of the regression line at $T = 1$. T is a dimensionless value which is the ratio of measured time over the end of consolidation time.

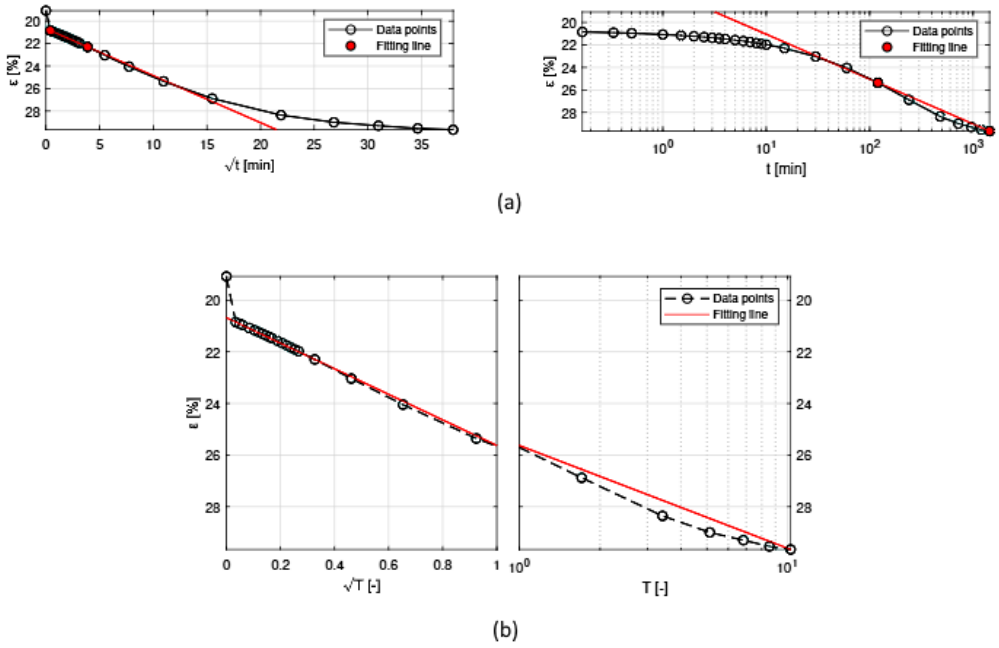

Figure 5.10: (a) Determination of two regression lines in $\sqrt{t} - \varepsilon_c$ and $\log(t) - \varepsilon_c$ in Test01 step 14. (b) The intersection of the regression line at $T = 1$. T is a dimensionless value which is the ratio of measured time over end of consolidation time.

In this discussion, both separation methods gives more accurate and certain results if the oedometer tests are performed with longer load duration. The results obtained from the 24 hr measurements (7.5 hrs and 2.26 hrs in ANACONDA and Brinch Hansen, respectively) will not be sufficient enough to consolidate in a super high plasticity clay such as Søvind Marl. Based on Grønbech et al. (2010) experience from the tests on Søvind Marl, it was found that the consolidation strains could be determined for at least 2 days each load step and this period was also found in this study in 14day load step tests.

5.3.1 Comparison of consolidation parameters results

Consolidation strains

The strain separation methods are used to separate the consolidation and creep strains as only the consolidation is used in the analysis. The results in all the tests (excluding the unloading incremental loads) are plotted in Figure 5.11.

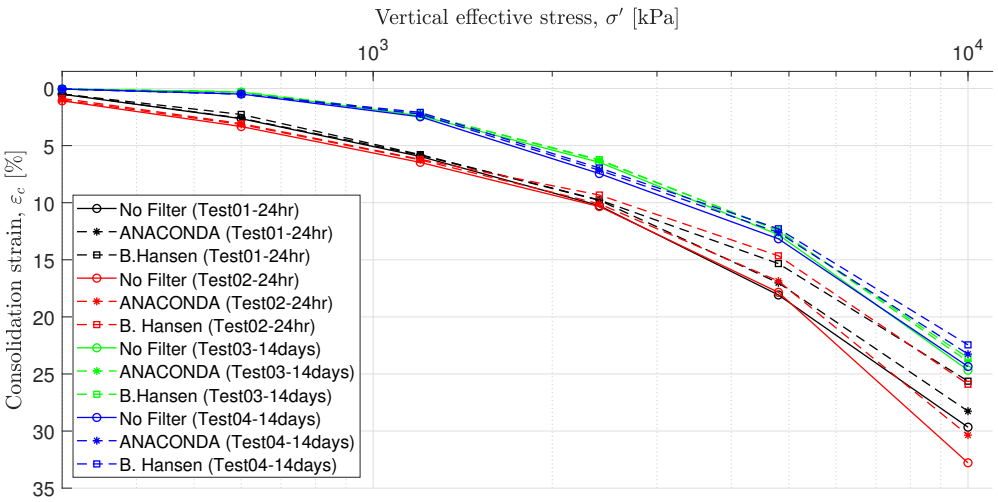

Figure 5.11: Comparison of the strain separation methods used in all test samples without unloading phase. No Filter curve is the stress-strain curve where there are no separation of strains applied.

As shown in Figure 5.11, the consolidation strains results in ANACONDA method and Brinch Hansen's method are almost identical in Test03 and Test04. However in Test01 and Test02 (24hr measurements), it is noticeable that Brinch Hansen has shifted upward at the second to the last step of the curve. This is because of the high values of creep strains obtained due to the steep slope in $\log(t) - \varepsilon_c$ graph as discussed in section 5.3, thus the consolidation strains becomes less.

This is also shown in the correlation analysis for Test01 and Test02 in Figure 5.12(a) and Figure 5.12(b) for Test03 and Test04. The consolidations strains are more scatterred in

Figure 5.12(a) than in Figure 5.12(b). Test03 and Test04 shows a very good fit that has correlation coefficient of approximately 1. However, the consolidations strains still presents a good corrrelation of 0.96 in Test01 and Test02.

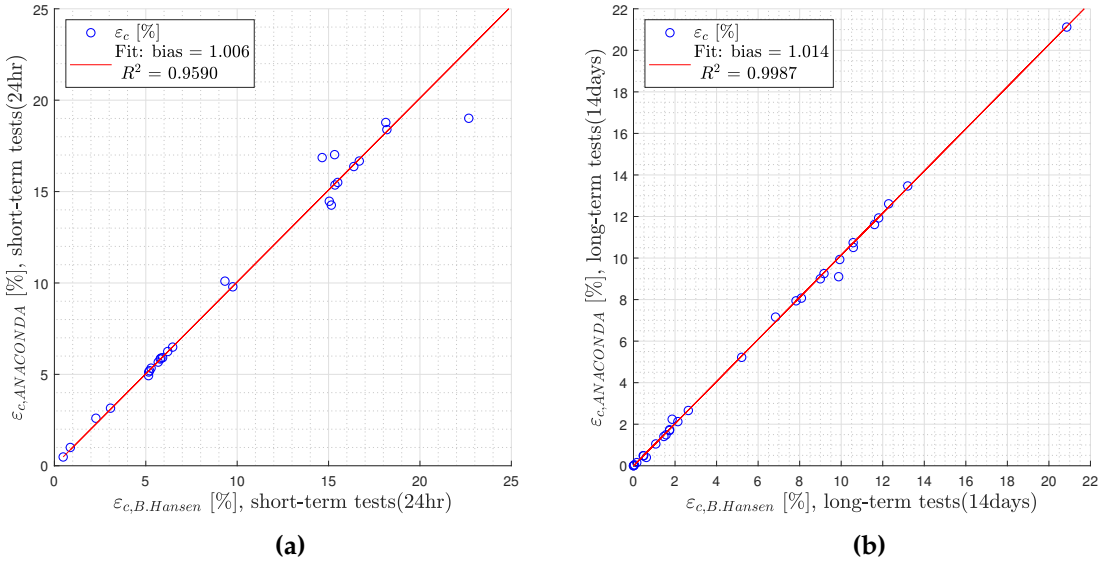

Figure 5.12: (a) Correlation between Brinch Hansen and ANACONDA on ε_c results for Test01 and Test02. (b) Correlation between Brinch Hansen and ANACONDA on ε_c results for Test03 and Test04.

Secondary compression index

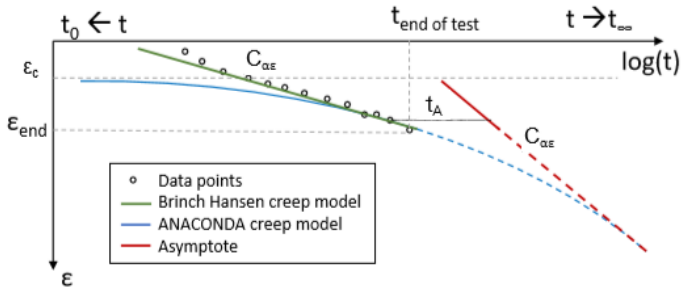

Figure 5.13: Difference of ANACONDA and Brinch Hansen approach in calculating $C_{\alpha\varepsilon}$, Parada (2017).

Figure 5.13 shows the different approach of ANACONDA and Brinch Hansen's method to calculate the secondary compression index $C_{\alpha\varepsilon}$. Brinch Hansen's method use the end tail of the data as a slope in order to obtain $C_{\alpha\varepsilon}$ while ANACONDA method does not use

the data itself to determined $C_{\alpha\varepsilon}$ but use an iteration process that predict the final state of creep defined by its asymptote. As secondary compression index $C_{\alpha\varepsilon}$ calculation is based on the slope of the end tail of the data in Brinch Hansen's method, the longer the duration of load step it is the lower the angle of the slope will be and therefore the $C_{\alpha\varepsilon}$ is also low.

The correlation between ANACONDA and Brinch Hansen method on $C_{\alpha\varepsilon}$ parameter in 24hr load step test is shown in Figure 5.14(a) while in 14day load step test is shown in Figure 5.14(b). Both shows a very good fit with a correlation of 0.94 and 0.93, respectively. It is clearly seen that using the ANACONDA method, the $C_{\alpha\varepsilon}$ values are higher than using the Brinch Hansen method.

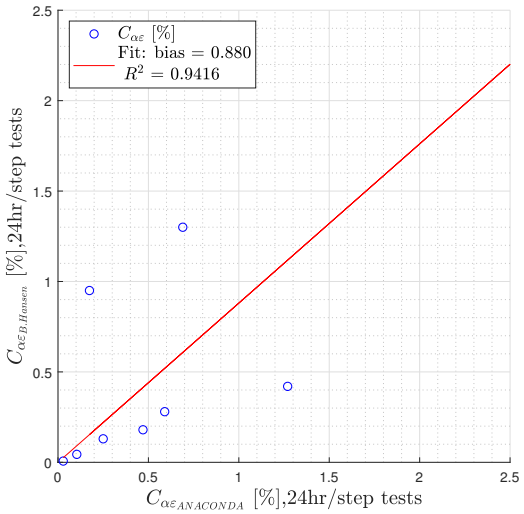

(a) Correlation of $C_{\alpha\varepsilon}$ for Test01 and Test02.

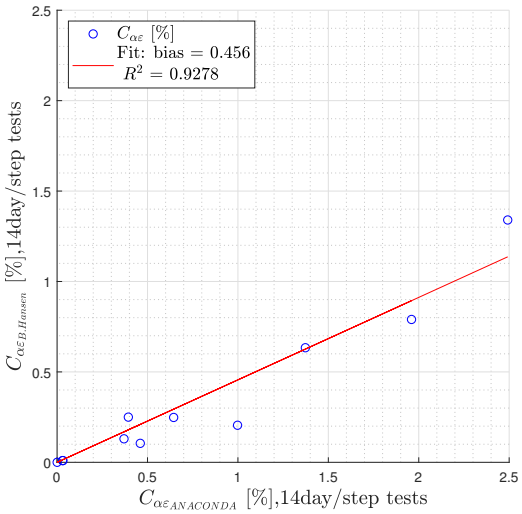

(b) Correlation of $C_{\alpha\varepsilon}$ for Test03 and Test04.

Figure 5.14

Consolidation modulus

The consolidation modulus M describes the stiffness of the soil when the effective stresses increases causing the increase in strains. The results of M in all the test samples (excluding the unloading phase) after the consolidation strains are isolated using the two separation strains methods used, can be shown in Figure 5.15. It can be seen that both ANACONDA and Brinch Hansen results are almost identical in each test, however there is a significant difference particularly at the lowest vertical mean stress level on the stiffness of the clay used in two different load duration tests. This is further discussed in section 5.4.1.

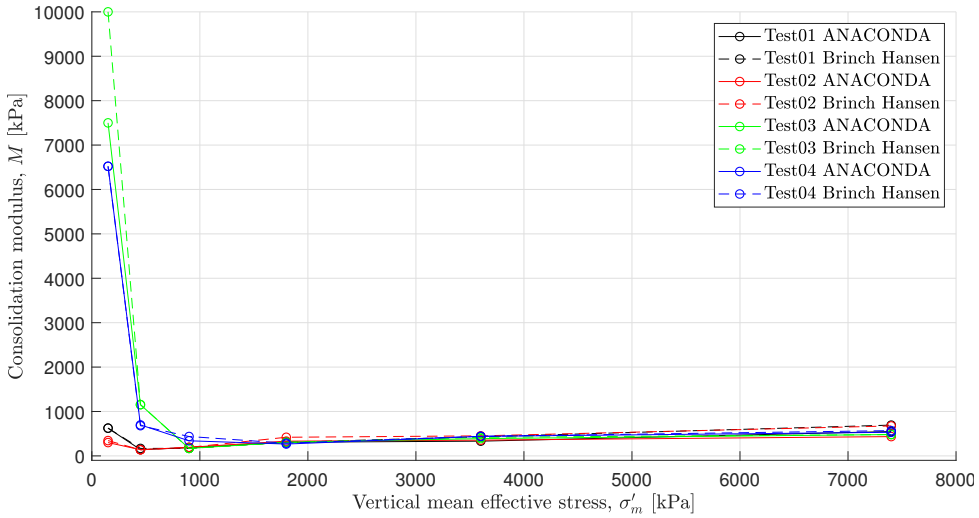

Figure 5.15: Outcome of consolidation modulus parameter in all test samples.

The correlation of consolidation moduli between the two methods used are more highly correlated in 14day load step tests which have a correlation coefficient of 0.97, see Figure 5.16(b) than in 24hr load step tests which has a correlation coefficient of 0.88, see Figure 5.16(a) .

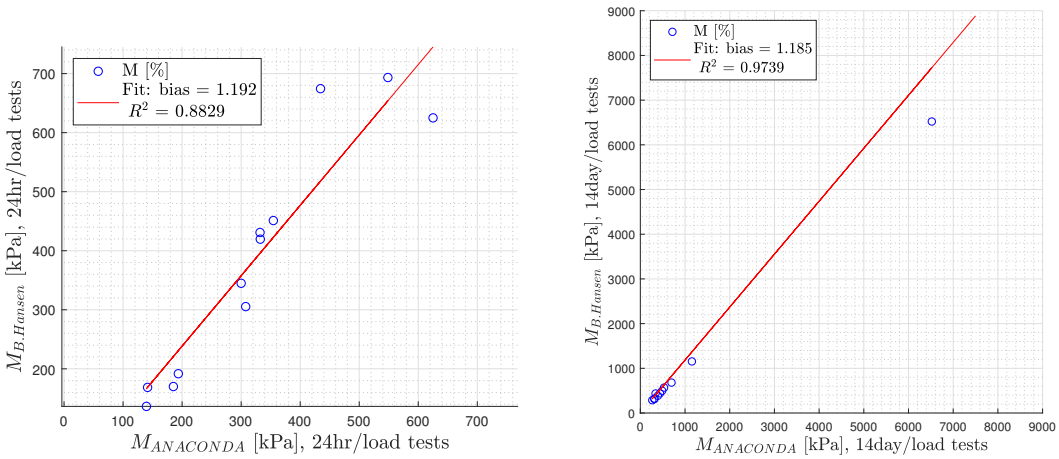

(a) **(b)**

Figure 5.16: Correlation between the two methods on M results for Test01 and Test02 (a) and for Test03 and Test04 (b).

Consolidation modulus has a consistent equation which has exactly one solution and therefore it depends on how the strains are separated. Based on the correlation analysis, the M values obtained by Brinch Hansen method are higher than ANACONDA method.

This make sense as the consolidation strains became more less after the creep was taken out from the total strains using Brinch Hansen's method than using ANACONDA method (see in the previous Figure 5.11).

5.4 Discussion on preconsolidation stress results

5.4.1 Issues in data interpretation using Janbu's method

The method involves plotting the σ_m against M, both in linear scale, as shown in Figure 5.17(a) and Figure 5.17(b) . As explained in Chapter 4, as σ_m increases, M suddenly drops and σ'_{pc} is obtained where the intersection of the slope of the descending part of the curve and the line of the minimum value of M. After σ'_{pc} is determined, M starts to increase and follows the m slope, see Figure 5.18.

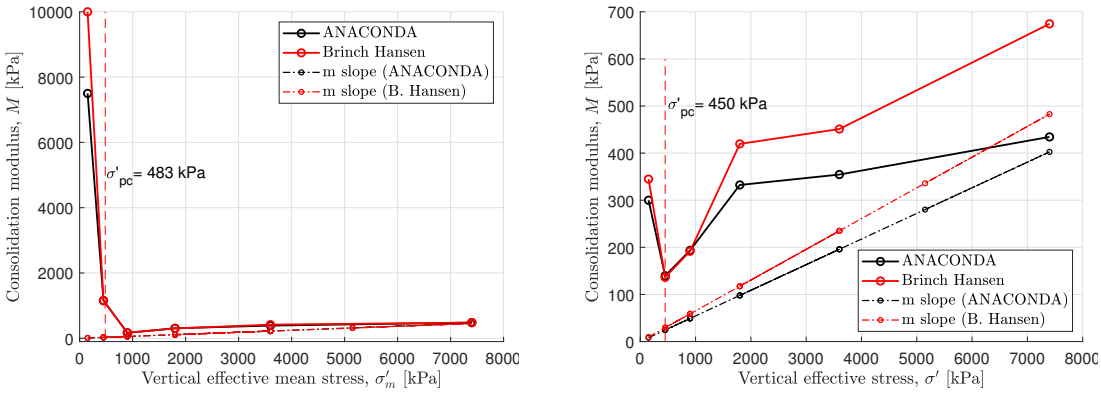

(a) Janbu method used in Test03.

(b) Janbu method used in Test02.

Figure 5.17

However, the outcome of σ_m vs. M in this thesis is not similar on the variation of Janbu's method for determining the σ'_{pc} shown in Figure 5.18. According to Janbu (1981), the shape of the σ_m vs. M varies depending on the soil type that is being investigated. These shapes are shown in Figure 5.19. Overconsolidated soils OC (a), tend to have a constant value of M between M_0 (highest M in OC state which is P_o in the figure below) and σ'_{pc} and then the curve will increase after it has reached the σ'_{pc}. In normally consolidated NC soils (b), M increases linearly with an increasing m slope when σ_m passes σ'_{pc}.

As seen in Figure 5.19, the σ_m vs. M in Figure 5.17(a) is markedly similar in OC type of soil (as in the case of Søvind Marl) in Figure 5.19(a). The only different is that, the curve does not increase after a slightly constant value of M where σ'_{pc} is determined. However, if the effective stress level was raised after 10MPa with a load increment ratio of 1 (i.e. the load

is doubled) in this thesis, this could possibly increases the M and will comprehensively determine the σ'_{pc}.

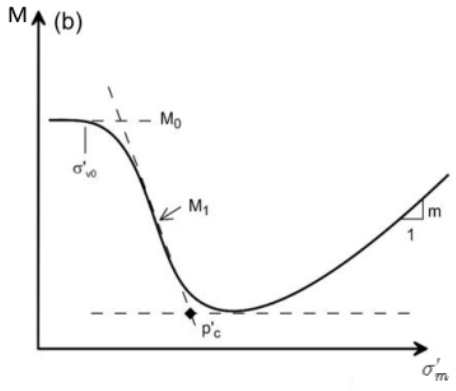

Figure 5.18: Janbu's method in determining preconsolidation stress (Lunne and Strandvik (1998)).

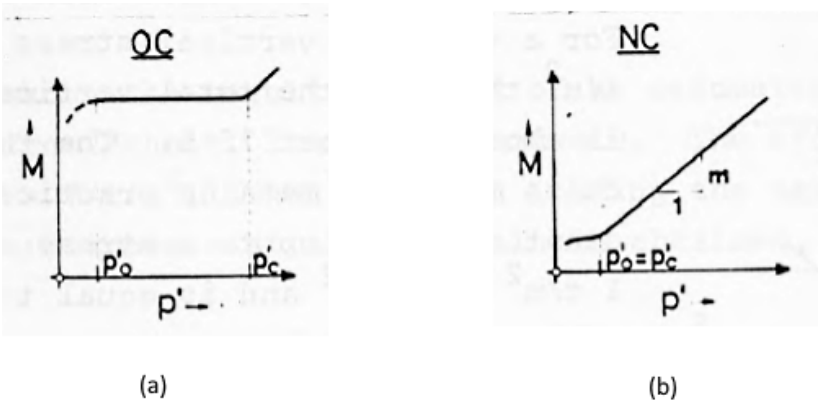

Figure 5.19: Different shapes of σ_m-M depending on the soil type. (a) $\sigma_{mean} - M$ for overconsolidated clay (b) $\sigma_m - M$ for normally consolidated clay (Janbu (1981)).

In addition, the σ'_{pc}=483 kPa found after following Janbus's concept is too low compared to what the other methods obtained. The gradual reduction of M is due to the fissures that closes during the loading process. This is also what Grønbech (2015) found when interperating the σ'_{pc} using Janbu's method.

However, the outcome of the $\sigma_m - M$ graph in 24hr measurement tests shown in Figure 5.17(b) for Test02, as an example, does not seems following the $\sigma_m - M$ concept as introduced by Janbu (1969) and the variation of $\sigma_m - M$ shapes in Janbu (1981)'s later paper. Here the convergence of the data points does not follow the m slope at all and due to this, it does not seem possible to interpret accurately the σ'_{pc}. This could maybe due to the quality of the soil or soil disturbance.

However, in order to confirm the discussions made in this section, a number of consolidation tests with an additional load step of effective stress more than 24 MPa have to perform on a very good soil sample quality in the future research in order to get a comprehensive description of the soil's past maximum stress σ'_{pc}.

5.4.2 Comparison of the preconsolidation stress results

The determined preconsolidation stress in all the tests are shown in Table 5.2 and the graphical comparison can be seen in Figure 5.20 for Test01 and Test02 (24 hr duration step) and Figure 5.21 for Test03 and Test04 (14 days duration step).

Methods	Test01 (24hr/load-step)		Test02 (24hr/load-step)		Test03 (14days/load-step)		Test04 (14days/load-step)	
	ANACONDA [kPa]	B. Hansen [kPa]	ANACONDA [kPa]	B. Hansen [kPa]	ANACONDA [kPa]	B. Hansen [kPa]	ANACONDA [kPa]	B. Hansen [kPa]
Janbu	450	450	450	450	483	483	472	472
Pacheco Silva	2508	2676	3053	3087	3088	2985	3240	2936
Jacobsen	4317	4314	5510	5168	6740	6485	6198	6400
Akai	4800-6100	4800-6300	4800-9500	4800-8450	4939-7465	5190-85056	4700-8209	4800-9200

Table 5.2: Preconsolidation stress results.

As shown in Figure 5.20 and Figure 5.21, the σ'_{pc} determined after the strain was separated using ANACONDA method (dashed-lines) and Brinch Hansen method (solid lines) has less influence on the results. However, the different preconsolidation methods used have an affect on the determined σ'_{pc} both in 24 hr load duration tests and 14 days load duration tests.

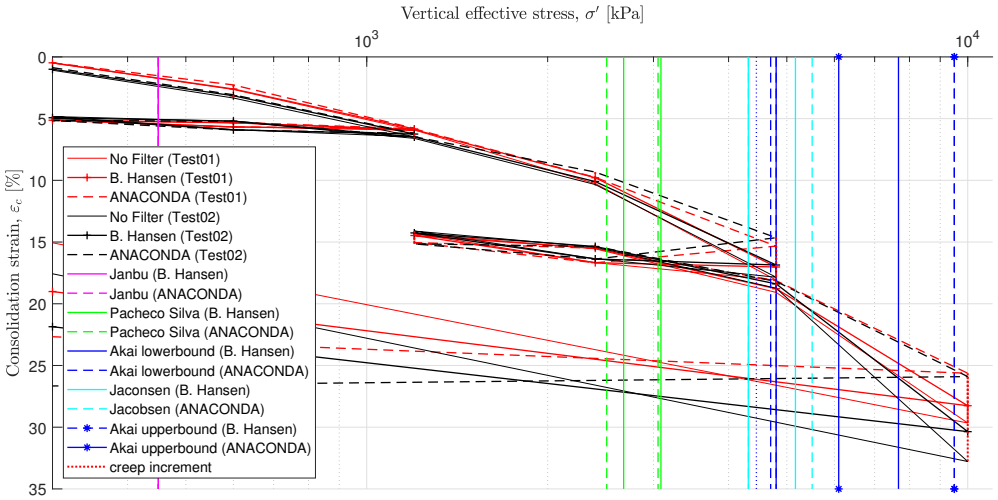

Figure 5.20: σ'_{pc} in Test01 and Test02. The vertical lines are the outcome of σ'_{pc} obtained from different methods. The σ'_{pc} values are presented in Table 5.2

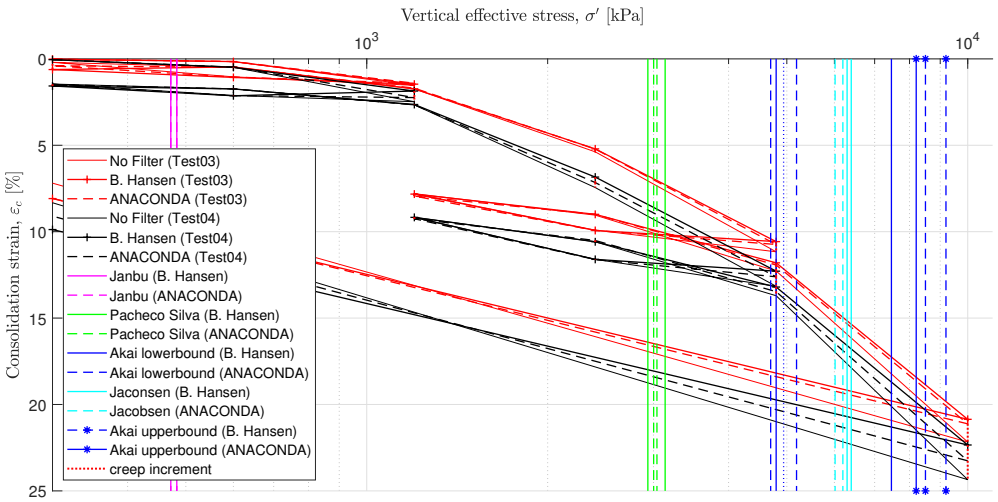

Figure 5.21: The determined σ'_{pc} in Test03 and Test04. The curves are the results from strain separation analysis and the vertical lines are the σ'_{pc} obtained from different methods. The σ'_{pc} values are presented in Table 5.2

As Søvind Marl had been preconsolidated due to its geological history and has already undergone a secondary consolidation with secondary compression index of up to 1% (Grønbech (2015)), it is then expected that σ'_{pc} has to be high. However, based on the values found in different methods, Janbu's method has the lowest value of σ'_{pc}. The lowest value determined was 450 kPa at 63 m depth (Test01 and Test02). As discussed in section 5.4.1, it was found that this value is due to the closure of the fissures and hereby not the "true" σ'_{pc}.

The second lowest σ'_{pc} was obtained by Pacheco Silva method which determined σ'_{pc} in a graphical way in $\log(\sigma') - \varepsilon_c$ curve and followed by lowerbound σ'_{pc} found by Akai method which shows some similarities. Akai's method (upper bound) has the highest value of σ'_{pc} obtained. However, the results in Jacobsen's method show a variation of σ'_{pc} values in all tests. The results shows more than 1000-1800 kPa in difference in 24hr load step tests and 14day load step tests.

In a previous study of Grønbech (2015), the lower bound of the preconsolidation stress due to the closure of fissures was found to be between 600 kPa and 800 kPa and the upper bound preconsolidation stress was found in a range of 6300 kPa to 9100 kPa, which is the true σ'_{pc}. These results are almost identical on the σ'_{pc} obtained in this study on the soil sample that was performed in 14day load step tests base on Akai and Jacobsen's results. In this thesis, the lower bound of the preconsolidation stress was found approximately 500 kPa while the upper bound preconsolidation stress was found in a range of approximately 4700 kPa to 9200 kPa.

Chapter 6

Conclusion

The main goal of this project was to investigate the effect of load duration on geotechnical parameters such as preconsolidation stress and swelling pressure in oedometer testing on overconsolidated highly plastic Søvind Marl. This clay was let to fully consolidate and let to resist the swelling during the testing and compared to the traditional 24 measurements.

First, the swelling pressure has been determined. It was argued in section 5.1.2 that the effect of load duration on swelling pressure will be investigated only on the soil samples used in long duration tests (Test03 and Test04) as the soil samples used in short duration test (Test01 and Test02) does not swell as was expected. These were expected to swell more due to its high plasticity and has less calcite content presents on these samples. Therefore the swelling pressure measured 24 hours after the tests in Test03 and Test04 were compared on the swelling pressure measured in long duration on these test samples. It was found that the soil samples still exhibited swelling after 24 hours and continued for an extended period of time. The stresses that completely resisted the swell pressure were 255 kPa (Test03) and 253 kPa (Test04). However, the measured swelling pressure after 24 hour measurements was only 208 kPa (Test03) and 195 kPa (Test04). Hence, 24 hour measurements underestimated the swelling pressure by 18-24%.

Furthermore, the consolidation test has been carried out. A series of load steps in two tests of different duration (where each load step were consolidated for 14 days and for 24 hours) were plotted in a continuous stress-strain graph. The stress-strain curves in 24hr measurements were 6% higher than the longer duration tests, contrary to what was expected. It was concluded that this occurs due to the spacing between fissures, wider on these samples (used in 24hr measurement tests) if compared to the samples used in longer duration tests, (see section 5.2). Fissures influenced the stiffness of the clay at lower stress. As the stress is increased, it forced the fissures to be closed and caused large

deformation from the first load step during testing. This became even more apparent as the data compilations progressed. Hence, the stress-strain curve in 24hr measurements is greater than the 14day load step tests.

When interpreting consolidation tests, only the consolidation strains were used in the analysis. In the separation of strains analysis, both ANACONDA and Brinch Hansen results were more accurate and certain if the oedometer tests had been performed for a longer duration. In 14day load step tests, both methods almost identically determined the complete consolidation, reached at approximately 2 days. However in 24hr measurements the full consolidation was determined in 7 to 8 hours (by ANACONDA) and 2.5 to 5 hours (by Brinch Hansen). In this investigation, it is concluded that the 24hr measurements are not sufficient to fully consolidate the overconsolidated and highly plastic clays. Thus underestimating the time at which the consolidation should be completed by 50%. Additionally, as the clay was not fully consolidated after 24 hours, this had wrongfully separated the total strains. Therefore the time at which the consolidation should be completed was underestimated by 85% when ANACONDA was used and by 95% when Brinch Hansen method was used.

In preconsolidation stress analysis, as expected, two preconsolidation stress at very different stress levels were determined which is often detected in on these types of clays. In the samples analysed, Janbu determined the lowest value of preconsolidation stress of approximately 500 kPa based on the gradual drop of consolidation modulus due to the closure of fissures. However this value is not related to preconsolidation events. Based on Akai and Pacheco Silva's results, there is no such effect on preconsolidation stress in two different duration tests. However, there was a variation on preconsolidation stresses obtained by Jacobsen's method. The preconsolidation stress was underestimated by 30-36% in 24hr measurement tests. In this study, the true preconsolidation stress was found in a range of approximately 4700-9200 kPa.

Overall, the goals of this project are considered to be fulfilled. Søvind Marl is considered as one of the complicated clay to deal with due to its high plasticity, fissured structure and categorized as highly overconsolidated clay therefore a proper load duration during oedometer testing is required when analysing such types of clays.

6.1 Recommendations and future work

In hindsight, a few parts of this study could have been approached differently. A few recommendations for future investigations on these type of clays are listed below:

- To get a satisfactory results in investigating the effect of load duration on stiffness parameters in oedometer testing on these type of clays, a numbers of test samples should be used in order to get a good comparison on the results. In this thesis, it is

impossible to compare the soil deformation (consolidation strains) in two different load duration tests in continuous stress-strain curve as the samples used in 24hr load step tests has wider spacing between the fissures that had influenced the stiffness of the clay. The comparison could be more clearer if the samples used has the same spacing of fissures in order to see the difference of the soil deformation when the load is applied. As the sample taken from 35 and 63 m depth behaved differently due to the effect of fissures, it could be better to test these soil samples in two different load durations each depth.

- To get a comprehensive description of the stiffness of Søvind Marl, high stresses are a necessity.
- For research purposes e.g. studying the development in creep properties, 14 days might be acceptable, but if it just to ensure that consolidation is 100% completed, this period is much to long.
- Finally, the salinity of water that is used in saturation should be equal on the salinity of the pore water in the specimen as it can be a factor that can effect the results of such laboratory tests.

References

Akai (1960). *De strukturellen Eigenschaften von schluft Mitteilugen (in German).* . K. Akai.

Bishop (1965). *Undisturbed samples of London clay from the ashford common shaft: Strength-effective stress relationships*. . Geoteknique.

Bjerrum (1967). *Engineering geology of Norwegian Normally-Consolidated Marine Clays as related to Settlements of Building*. 1. ed. Laurits Bjerrum.

Brinch Hansen (1961). *A Model Law for Simultaneous Primary and Secondary Consolidation*. 7. ed. Geoteknisk Institut.

Casagrande (1932). *Research on the Atterberg Limits of Soils.* 8th. A. Casagrade.

DS (ISO/TS 17892-5). *Incremental loading oedometer test*. . Danish Standard.

Geoviden (2010). *Danmark's geologiske udvikling fra 65 til 2.6 mio. år før nu*.

Google map (2019). *location of aarhus lighthouse*. Visited 2019-25-09. URL: https://www.google.com/maps/place/Light+House,+8000+Aarhus/@56.165628,10.2291673,17z/data=!3m1!4b1!4m5!3m4!1s0x464c3fa0d73943bd:0x46951d290b3c412c!8m2!3d56.165628!4d10.231356.

Grønbech, Gitte Lyng (2014). "Geotechnical properties of Søvind Marl- a plastic Eocene clay". In:

– (2015). "Søvind Marl behavior of a plastic fissured Eocene clay". In:

Grønbech, Gitte Lyng, Lars Bo Ibsen, and Benjaminn Nordahl Nielsen (2010). "Determination of the deformation properties of søvind Marl". In:

Grønbech, Gitte Lyng, Lars Bo Ibsen, and Benjaminn Nordahl Nielsen (2013). "Interpretation of Consolidation test on Tertiary Clay". In:

Grønbech, Gitte Lyng, Lars Bo Ibsen, and Benjamin Nordahl Nielsen (2014). "Comparison of Liquid Limit of highly plastic clay by means of Casagrande and Fall Cone Apparatus". In:

Holtz, W.G. (1983). "The influence of vegetation on the swelling and shrinking of clays in the United States of America". In:

Jacobsen (1992). *Bestemmelse af forbelastningstryk i laboratoriet.* . H. Moust Jacobsen.

Janbu (1969). *The resistance concept applied to deformation of soils*. . N. Janbu.

– (1981). *Settlement Calculations based on the Tangent Modulus Concept Part 1*. . N. Janbu.

John D. Nelson (2015). *Foundation Engineering for Expansive Soils.* . John Wiley and Sons Incorporated.

Kaufmann, Kristine Lee (2010). "Strength and deformation properties of a tertiary clay at Moesgaard Museum". Aalborg University.

Lunne T., Berre T. and S. Strandvik (1998). "Sample disturbance effects in deepwater soil investigations". In:

Okkels, N. and P. B. Hansen (2016). "Swell pressure and yield stresses in Danish, highly overconsolidated, Palaeogene clays of extreme plasticity". In:

Pacheco Silva (1970). *A new graphical construction for determination of the preconsolidation stress of a soil sample.* . F. Pacheco Silva.

Parada, Juan (2017). "Comparative analysis on the methods for determination of consolidation and creep parameters using custom software". Aalborg University.

Simonsen, T (2017). "Scientist combat a tricky soil - Science Nordic". In:

Skempton (1969). *Joints and fissures in London clay at wraysbury and esdware.* . Geoteknique.

Terzaghi, Charlez (1925). "Principles of soil Mechanics: IV- Settlement and Consolidation of Clay". In:

Thøgersen, L (2001). "Effects of experimental techniques and osmotic pressure on measured behavior". In:

Wikipedia (2013). *Soil Consolidation*. Visited 2020-23-12. URL: https://en.wikipedia.org/wiki/Soil_consolidation.

Appendix A

Consolidation parameters

A.0.1 Consolidation modulus

The consolidation modulus M is a stiffness parameter given by equation A.1. The consolidation modulus increases in time during the consolidation of soil (after the preconsolidation stress is obtained) as the the soil becomes stiffer as load increasing.

$$M = \frac{\Delta\sigma'}{\Delta\varepsilon_c} \tag{A.1}$$

Where:

$\Delta\sigma'$	Effective stress difference in the previous and current stress applied	[kPa]
$\Delta\varepsilon_c$	Strain difference in the previous and current strain applied	[%]

A.0.2 Compression and recompression index

The compression index C_c is the slope taken from virgin compression curve and is used to find the settlement in *NC* soil. While the recompresssion index C_r is the slope taken from the first loading and reloading of the stress-strain curve shown in Figure A.1 which is used to find the consolidation settlement for *OC* soil.

The slope of the compression index C_c and recompression index C_r gives the characteristic relation between stress applied and the change in deformation when compressing the soil. The equation (A.2) is used to determined both C_c and C_r.

$$C_c = \frac{\Delta\varepsilon}{\Delta\log(\sigma')} \tag{A.2}$$

where:

$\Delta\varepsilon$	the change in strain along the compression or compression line [%]
$\Delta \log(\sigma')$	the change in $\log(\sigma')$ along the compression or compression line [%]

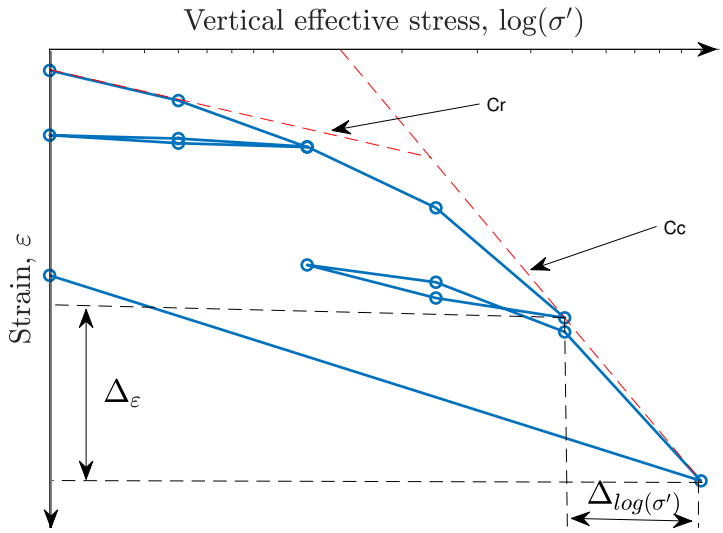

Figure A.1

.

A.0.3 Coefficient of consolidation, coefficient of permeability and degree of consolidation

The definition of these parameters are described below:

- The coefficient of consolidation c_v - tells the rate of the consolidation process. This is measured in m^2/s.
- Coefficient of permeability k - defined as the flow velocity of the soil undergoes consolidation and is also commonly reffered as the hydraulic conductivity of soil. This is expressed in m/s.
- Degree of consolidation U - is the ratio of the amount of consolidation at any time to the final consolidation obtained under a given stress condition. This is expressed in %.

These parameters are dependent on the dimensionless time factor T_v and is given by equation A.3.

$$T_v = \frac{c_v}{H_D^2} t = \frac{kM}{\gamma_w H_D^2} t \tag{A.3}$$

where:

H_D^2	the drainage path [m]
M	consolidation modulus [kPa]
γ_w	specific weight of water $[\mathrm{kN/m^3}]$

The expression used to compute U is given by equation A.4. If the consolidation is 50% done (time = 50 t_50), U= 0.5, it was found that the time factor T_v = 0.2. By applying this to equation A.3, the c_v is obtained given in equation A.5. While k is dependent on c_v, γ_w and M, the parameter k can also be derived from equation A.3 which is given in equation A.6.

$$U = 1 + \frac{1}{2}T^{-}3 \tag{A.4}$$

$$c_v = \frac{TH_D^2}{t} = 0.2\frac{H_D^2}{t_{50}} \tag{A.5}$$

$$k = \frac{c_v \gamma_w}{M} \tag{A.6}$$

Appendix B

Time vs. natural strain plots

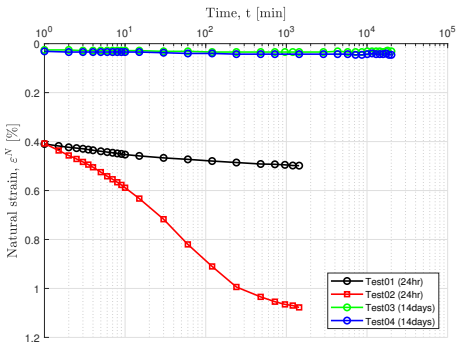

(a) Step 1

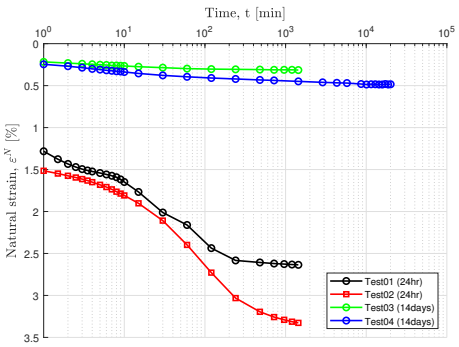

(b) Step 2

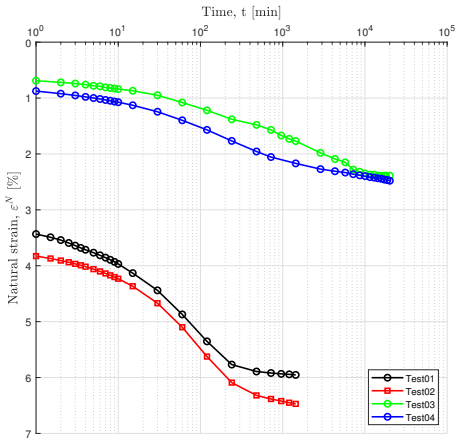

(a) Step 3

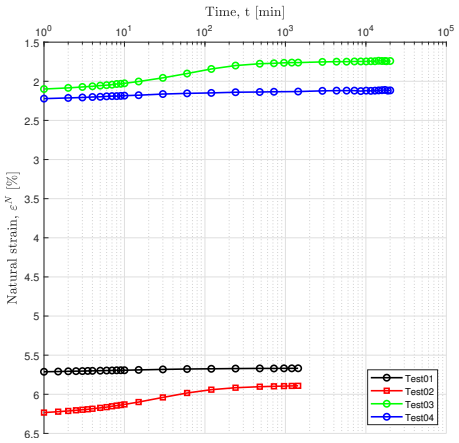

(b) Step 4

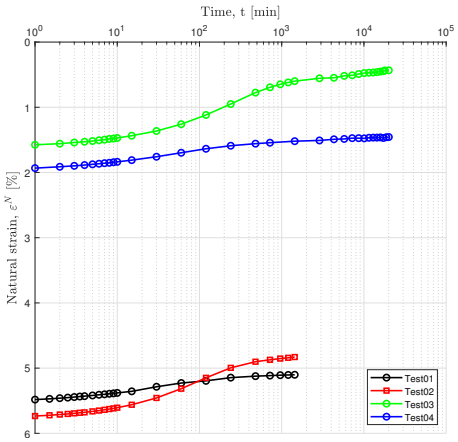

(a) Step 5

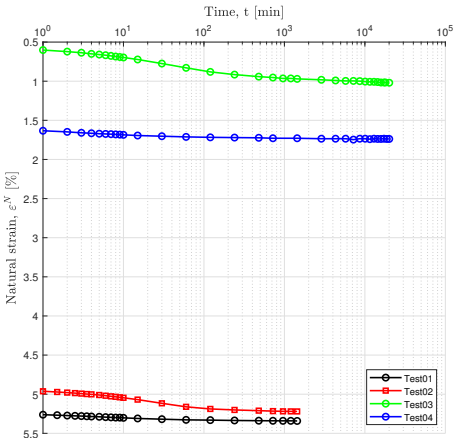

(b) Step 6

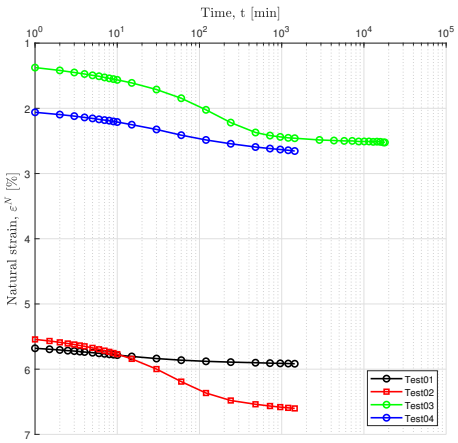

(a) Step 7

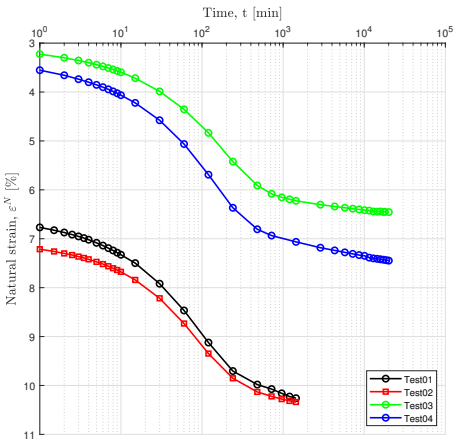

(b) Step 8

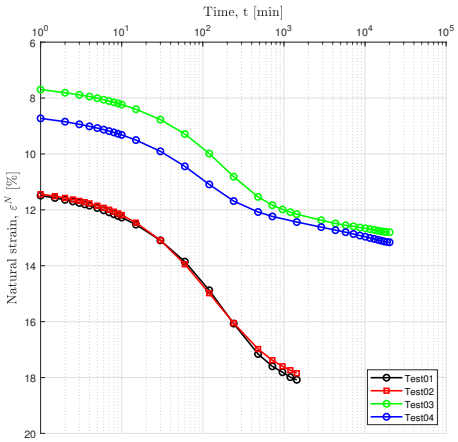

(a) Step 9

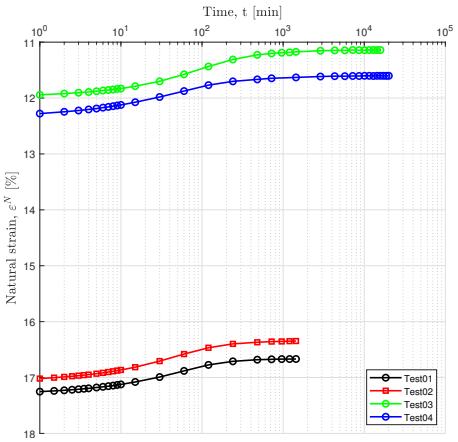

(b) Step 10

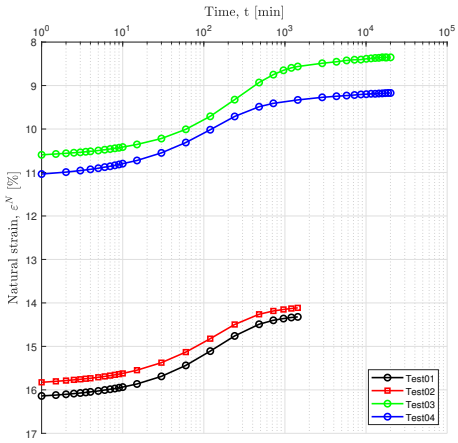

(a) Step 11

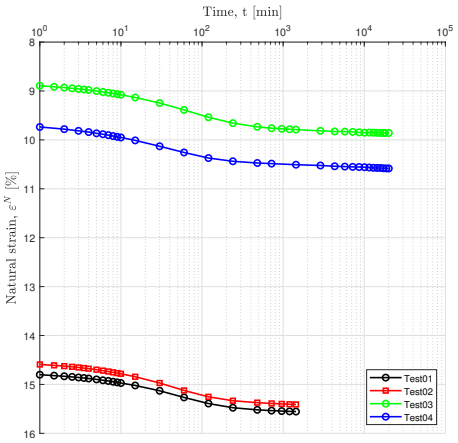

(b) Step 12

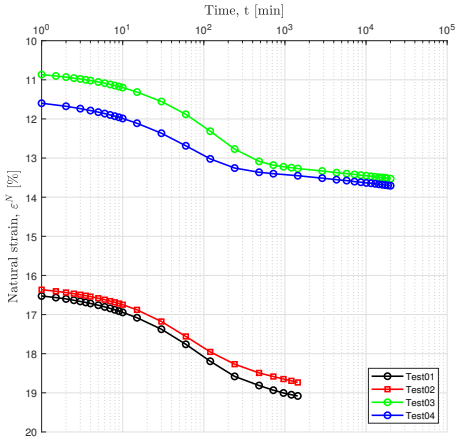

(a) Step 13

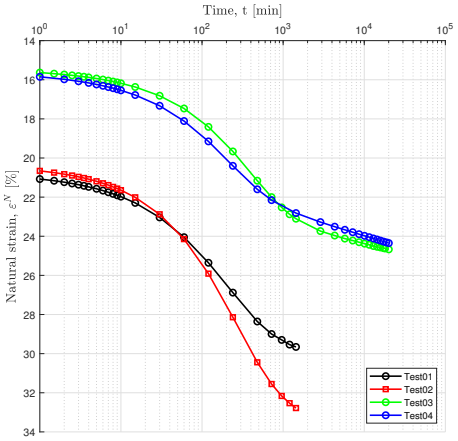

(b) Step 14

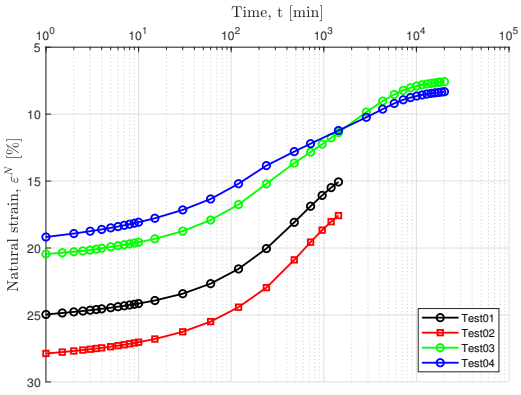

(a) Step 15

Stress-strain plot for all the tests sample

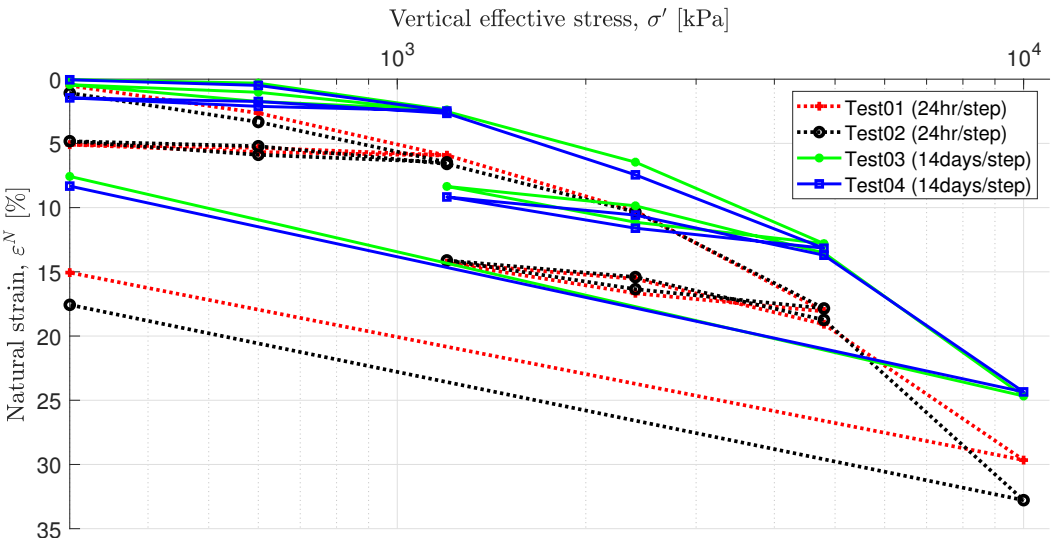

Figure B.9: Consolidation curves of the four samples which will be use in data analysis

Appendix C

Strain separation results

In this appendix the results from strain separation analysis are presented. The outcome of each test is illustrated in a graph and below the plot the parameters obtained are presented in tables.

C.0.1 Test01

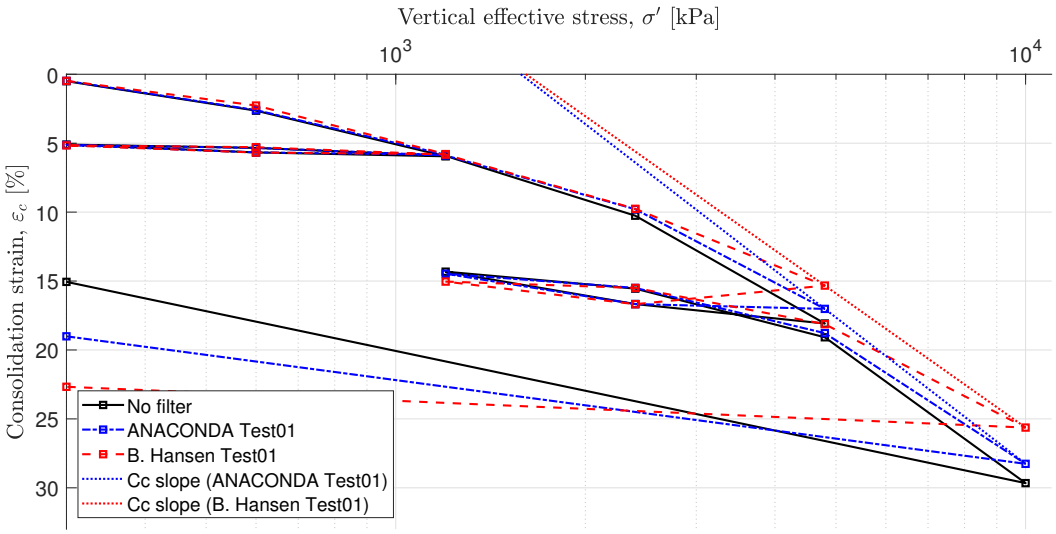

Figure C.1: Virgin compression index C_c Test01.

Step	σ [kPa]	ε_c [%]	e_c [-]	ε_{creep} [%]	ε_{tot} [%]	M [kPa]	$C_{\alpha\varepsilon}$ [%]
1	300	0.485	1.193	0.014	0.50	625	0.03
2	600	2.60	1.15	0.04	2.64	141.5	0.104
3	1200	5.85	1.078	0.11	5.95	185.19	0.25
4	600	5.67	1.08	-0.005	5.67	3529	-0.012
5	300	5.13	1.095	-0.03	5.10	555.56	-0.08
6	600	5.34	1.09	0.005	5.34	1429	0.013
7	1200	5.89	1.08	0.023	5.92	1091	0.066
8	2400	9.79	0.99	0.48	10.26	307.69	1.27
9	4800	17.024	0.83	1.07	18.08	331.95	3.10
10	2400	16.67	0.84	-0.006	16.67	6857	-0.02
11	1200	14.47	0.98	-0.15	14.32	545.45	-0.44
12	2400	15.51	0.87	0.05	15.56	1154	0.133
13	4800	18.78	0.79	0.30	19.08	733.45	0.87
14	10000	28.26	0.58	1.42	29.66	548.52	4.11
15	300	19.01	0.79	-3.97	15.06	1049	-11.49

Table C.1: Parameter results of Test01 using ANACONDA method.

Step	σ [kPa]	ε_c [%]	e_c [-]	ε_{creep} [%]	ε_{tot} [%]	M [kPa]	$C_{\alpha\varepsilon}$ [%]
1	300	0.48	1.197	0.02	0.50	625	0.007
2	600	2.56	1.15	0.07	2.64	168.54	0.045
3	1200	5.79	1.08	0.16	5.95	169.97	0.13
4	600	5.69	1.082	-0.02	5.67	6000	-0.008
5	300	5.16	1.09	-0.06	5.10	566.04	-0.04
6	600	5.29	1.091	0.05	5.34	2307	0.019
7	1200	5.83	1.08	0.08	5.92	1111	0.04
8	2400	9.76	0.99	0.50	10.26	305.34	0.42
9	4800	15.34	0.87	2.75	18.08	430.88	2.59
10	2400	16.68	0.84	-0.01	16.67	-1778	-0.008
11	1200	15.04	0.88	-1.03	14.32	731.71	-0.99
12	2400	15.50	0.87	0.06	15.56	2609	0.05
13	4800	18.13	0.80	0.95	19.08	912.55	0.82
14	10000	25.63	0.64	4.03	29.66	693.33	3.99
15	300	22.67	0.71	-2.89	15.06	3277	-2.09

Table C.2: Parameter results of Test01 using Brinch Hansen method.

C.0.2 Test02

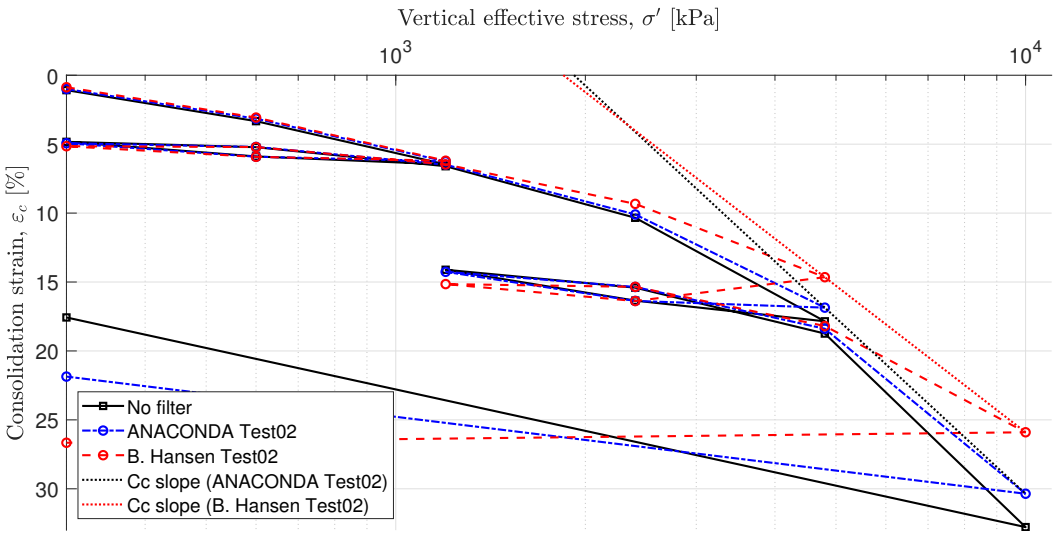

Figure C.2: Virgin compression index C_c Test01.

Step	σ [kPa]	ε_c [%]	e_c [-]	ε_{creep} [%]	ε_{tot} [%]	M [kPa]	$C_{\alpha\varepsilon}$ [%]
1	300	1.00	1.145	0.08	1.08	300	0.174
2	600	3.15	1.10	0.18	3.33	139.53	0.47
3	1200	6.25	1.03	0.22	6.47	193.55	0.59
4	600	5.91	1.039	-0.02	5.89	1765	-0.04
5	300	4.94	1.06	-0.11	4.83	306.12	-0.28
6	600	5.20	1.054	0.02	5.22	1111	0.04
7	1200	6.49	1.03	0.12	6.6	465.12	0.27
8	2400	10.10	0.95	0.24	10.34	332.41	0.69
9	4800	16.87	0.80	0.98	17.85	354.51	2.84
10	2400	16.37	0.81	-0.03	16.35	4898	-0.08
11	1200	14.26	0.86	-0.15	14.11	566.04	-0.43
12	2400	15.36	0.83	0.05	15.41	1091	0.14
13	4800	18.39	0.77	0.34	18.74	792.08	0.99
14	10000	30.36	0.51	2.44	32.78	434.42	7.06
15	300	21.86	0.69	-4.31	17.57	1141	-12.48

Table C.3: Parameter results of Test02 using ANACONDA method.

Step	σ [kPa]	ε_c [%]	e_c [-]	ε_{creep} [%]	ε_{tot} [%]	M [kPa]	$C_{\alpha\varepsilon}$ [%]
1	300	0.87	1.148	0.21	1.08	344.83	0.095
2	600	3.07	1.10	0.25	3.33	136.36	0.18
3	1200	6.20	1.03	0.27	6.47	191.69	0.26
4	600	5.92	1.039	-0.025	5.89	2143	-0.02
5	300	5.15	1.06	-0.44	4.83	384.62	-0.41
6	600	5.21	1.054	0.01	5.22	5000	0.008
7	1200	6.47	1.03	0.13	6.6	472.44	0.11
8	2400	9.33	0.96	1.42	10.34	419.58	1.30
9	4800	14.65	0.85	3.66	17.85	451.58	3.08
10	2400	16.38	0.81	-0.04	16.35	-13873	-0.03
11	1200	15.15	0.84	-1.08	14.11	975.61	-0.75
12	2400	15.35	0.83	0.06	15.41	6000	0.05
13	4800	18.19	0.77	0.55	18.74	845.07	0.53
14	10000	25.90	0.61	6.34	32.78	674.45	5.87
15	300	26.66	0.59	-2.30	17.57	-1276	-1.24

Table C.4: Parameter results of Test02 using Brinch Hansen method.

C.0.3 Test03

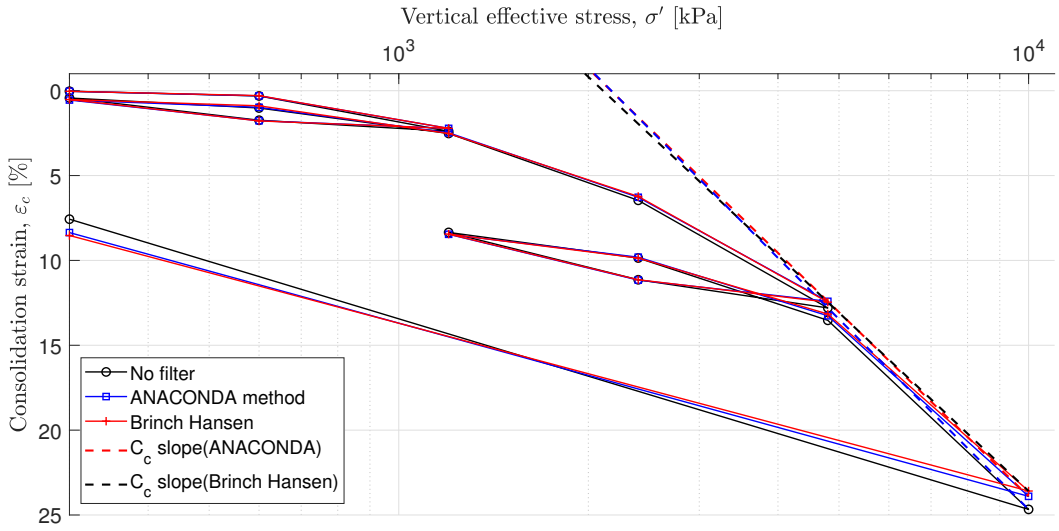

Figure C.3: Virgin compression index C_c of Test03. No filter curve is the $log(\sigma) - \varepsilon^N$ curve where no strain separation is applied.

Step	σ [kPa]	ε_c [%]	e_c [-]	ε_{creep} [%]	ε_{tot} [%]	M [kPa]	$C_{\alpha\varepsilon}$ [%]
1	300	0.037	1.118	-0.006	0.031	7500	-0.014
2	600	0.30	1.113	0.01	0.315	1154	0.032
3	1200	2.22	1.072	0.19	2.39	477.33	0.46
4	600	1.77	1.08	-1.03	1.74	169	-0.016
5	300	0.55	1.110	-0.208	0.43	1250	-0.30
6	600	0.98	1.098	0.044	1.02	697.67	0.11
7	1200	2.48	1.07	0.04	2.52	392.15	0.115
8	2400	6.28	0.99	0.19	6.46	306.90	0.37
9	4800	12.41	0.86	0.41	12.80	388.97	0.998
10	2400	11.16	0.88	-0.02	11.14	1904	-0.030
11	1200	8.46	0.94	-0.12	8.35	472.44	-0.287
12	2400	9.81	0.91	0.05	9.86	869.57	0.106
13	4800	13.26	0.84	0.27	13.53	693.64	0.28
14	10000	23.84	0.61	0.79	24.67	481.04	1.96
15	300	8.36	0.94	-0.82	7.57	621	-2.14

Table C.5: Parameter results of Test03 using ANACONDA method.

Step	σ [kPa]	ε_c [%]	e_c [-]	ε_{creep} [%]	ε_{tot} [%]	M [kPa]	$C_{\alpha\varepsilon}$ [%]
1	300	0.034	1.118	0.000006	0.031	10000	2.22e-18
2	600	0.29	1.112	0.02	0.315	1154	0.0095
3	1200	2.22	1.072	0.17	2.39	167.6	0.105
4	600	1.76	1.08	-1.03	1.74	1250	-0.015
5	300	0.52	1.108	-0.09	0.43	236.22	-0.06
6	600	0.89	1.1	0.012	1.02	681.82	0.05
7	1200	2.52	1.07	-0.000005	2.52	402.68	-1.243e-14
8	2400	6.23	0.99	0.226	6.46	300.75	0.13
9	4800	12.46	0.85	0.34	12.80	418.12	0.205
10	2400	11.14	0.88	0.0000001	11.14	2759	7.02e-15
11	1200	8.45	0.94	-0.096	8.35	468.75	-0.065
12	2400	9.86	0.91	-0.000002	9.86	869.57	1.101e-14
13	4800	13.16	0.84	0.36	13.53	733.95	0.19
14	10000	23.59	0.61	1.07	24.67	480.15	0.79
15	300	8.53	0.94	-0.95	7.57	632	-0.71

Table C.6: Parameter results of Test03 using Brinch Hansen method.

C.0.4 Test04

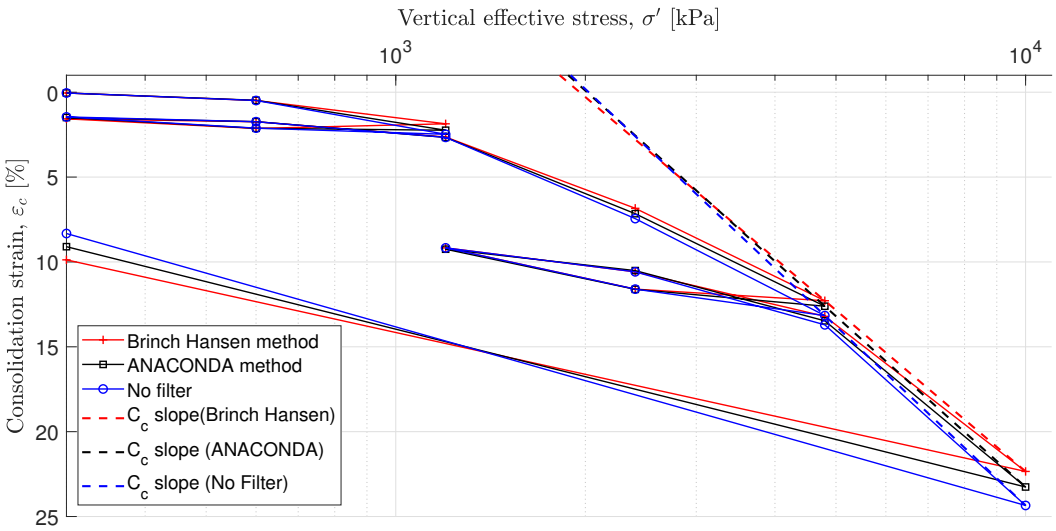

Figure C.4: Virgin compression index C_c and Recompression index C_r of Test04. No filter curve is the $log(\sigma) - \varepsilon^N$ curve where no strain separation is applied.

Step	σ [kPa]	ε_c [%]	e_c [-]	ε_{creep} [%]	ε_{tot} [%]	M [kPa]	$C_{\alpha\varepsilon}$ [%]
1	300	0.046	1.097	0.0001	0.046	6522	0.004
2	600	0.476	1.088	0.012	0.487	697.67	0.0303
3	1200	2.24	1.051	0.240	2.48	340.14	0.3940
4	600	2.125	1.053	-0.009	2.116	5217	-0.018
5	300	1.491	1.067	-0.031	1.456	473.19	-0.075
6	600	1.735	1.062	0.002	1.74	1230	0.003
7	1200	2.26	1.042	0.004	2.66	648.65	0.006
8	2400	7.16	0.948	0.304	7.45	266.85	0.646
9	4800	12.61	0.833	0.568	13.16	440.12	1.374
10	2400	11.614	0.854	-0.014	11.60	2410	-0.027
11	1200	9.254	0.903	-0.087	9.171	507.61	-0.205
12	2400	10.51	0.877	0.073	10.58	952.38	0.119
13	4800	13.47	0.815	0.233	13.71	810.81	0.343
14	10000	23.26	0.610	1.118	24.35	531.15	2.49
15	300	9.21	0.905	-0.918	8.33	685.08	-2.30

Table C.7: Results from analysis of Test04 using ANACONDA method.

Step	σ [kPa]	ε_c [%]	e_c [-]	ε_{creep} [%]	ε_{tot} [%]	M [kPa]	$C_{\alpha\varepsilon}$ [%]
1	300	0.045	1.097	0.0006	0.046	6522	0.0002
2	600	0.46	1.088	0.028	0.487	680.27	0.006
3	1200	1.90	1.058	0.570	2.48	436.68	0.250
4	600	2.14	1.053	-0.019	2.12	-2190	-0.007
5	300	1.57	1.065	-0.112	1.46	529.10	-0.046
6	600	1.74	1.061	-2.80e-14	1.74	1744	-9.015e-15
7	1200	2.64	1.043	0.017	2.66	666.67	0.007
8	2400	6.96	0.952	0.49	7.45	285.71	0.248
9	4800	11.79	0.851	1.373	13.16	440.77	0.634
10	2400	11.60	0.855	2.22e-13	11.60	3514	9.488e-14
11	1200	9.17	0.906	6.93e-14	9.171	493.62	3.935e-14
12	2400	10.58	0.875	0	10.58	849.26	1.253e-16
13	4800	13.20	0.821	0.503	13.71	916.03	0.215
14	10000	22.06	0.635	2.29	24.35	568.93	1.34
15	300	9.88	0.89	-1.55	8.33	778.05	-0.816

Table C.8: Results from analysis of Test04 using Brinch Hansen method.

Method	Test01 C_c [%]	Test02 C_c [%]	Test03 C_c [%]	Test04 C_c [%]
Brinch Hansen	32.29	35.29	36.04	31.55
ANACONDA	35.24	42.32	34.91	33.41
No Filter	36.31	46.85	34.53	35.10

Table C.9: Determined compression index C_c.

Appendix D

Preconsolidation stress results

In this Appendix, the results of the preconsolidation stress using different methods are presented.

D.1 Akai method results

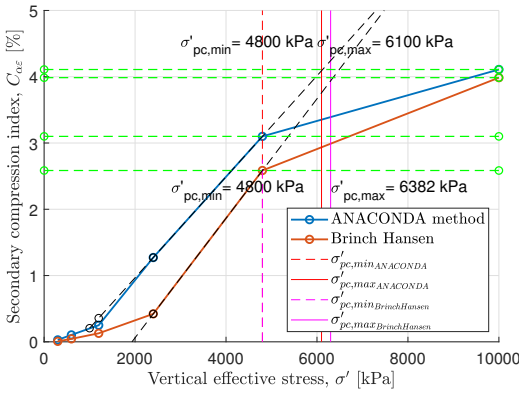

(a) Test01

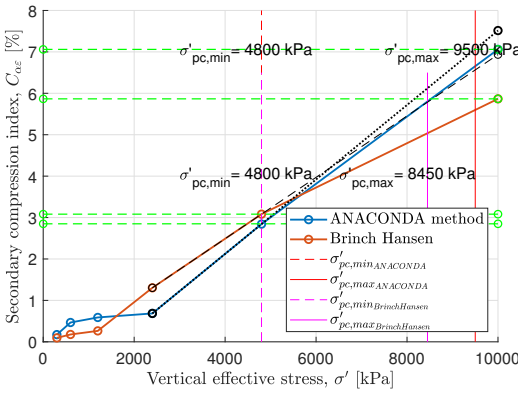

(b) Test02

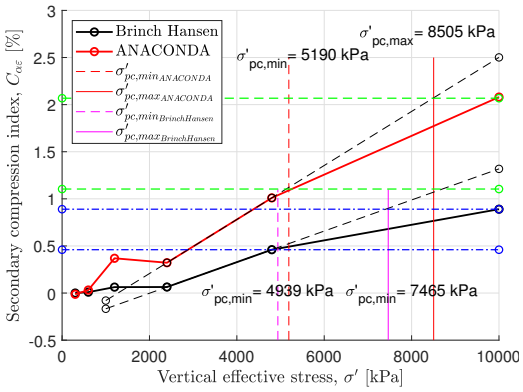

(a) Test03

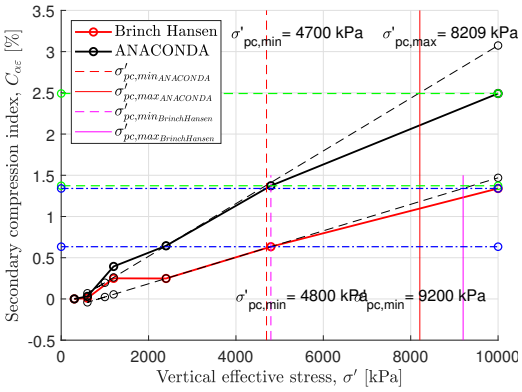

(b) Test04

D.2 Janbu method results

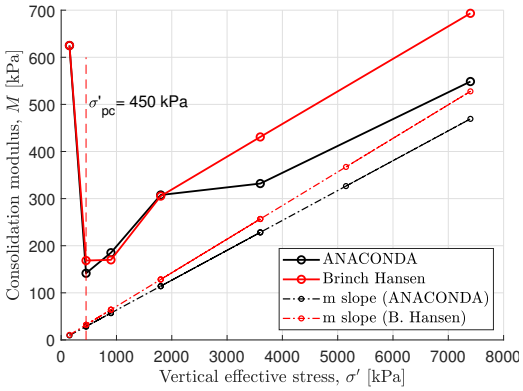

(a) Test01

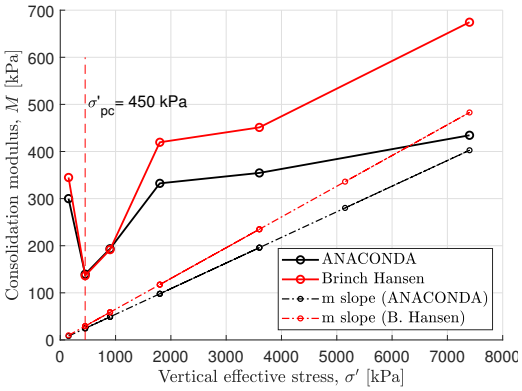

(b) Test02

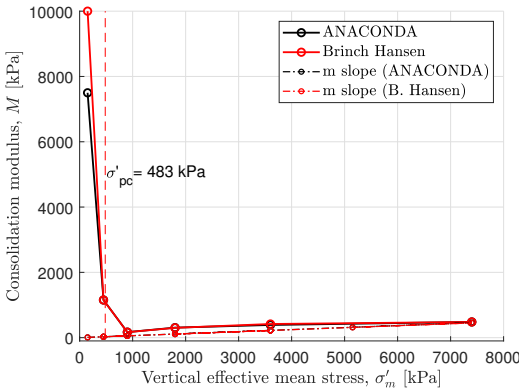

(a) Test03

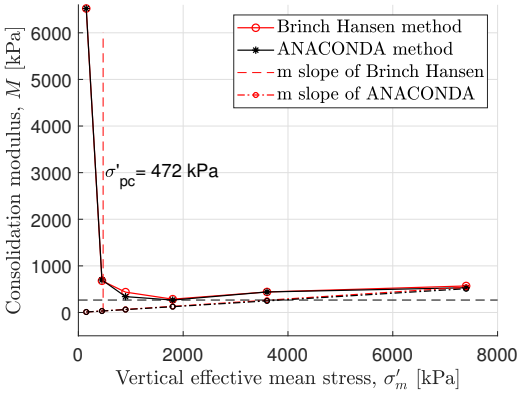

(b) Test04

D.3 Pacheco Silva method results

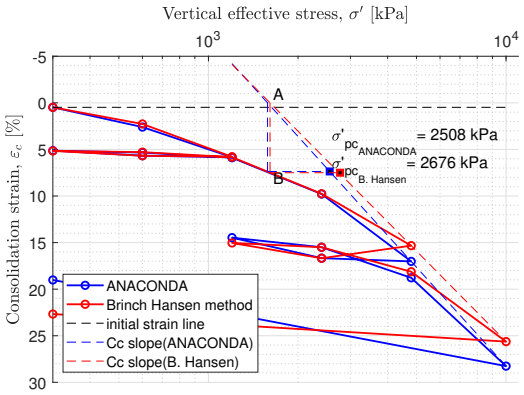

(a) Test01

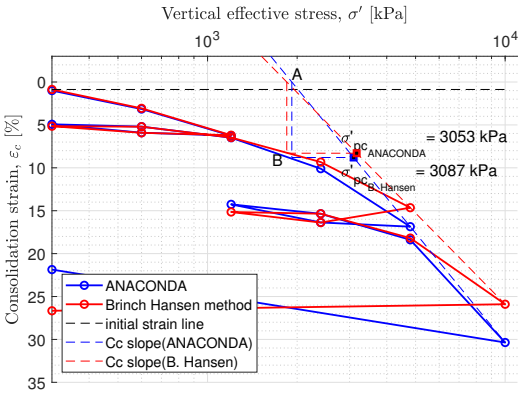

(b) Test02

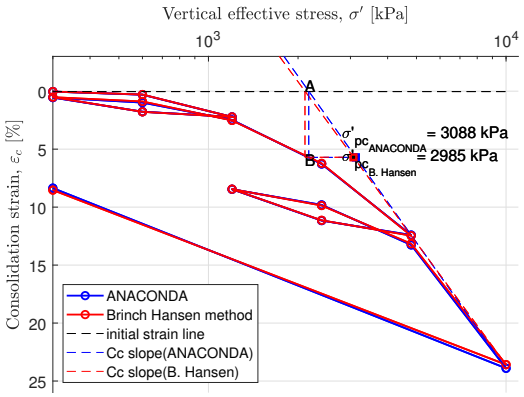

(a) Test03

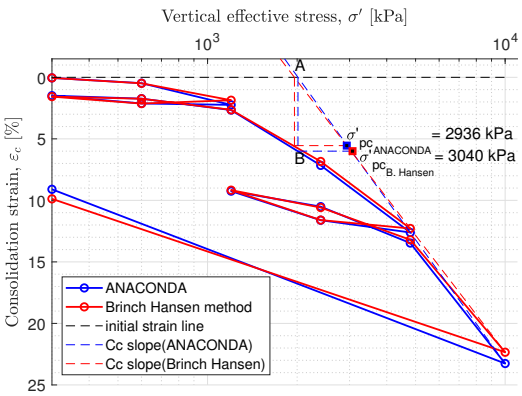

(b) Test04

D.4 Jacobsen method results

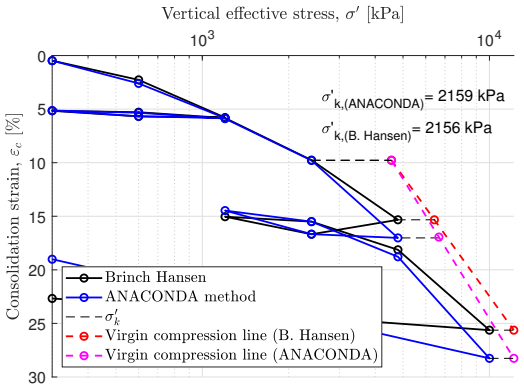

(a) Test01

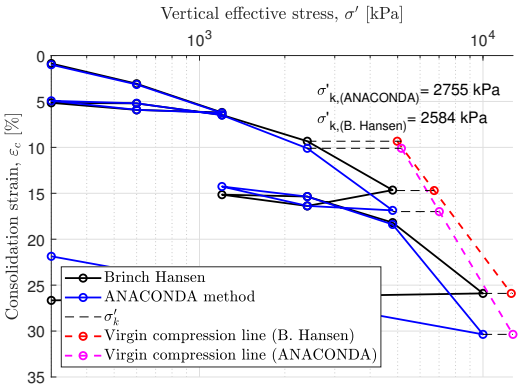

(b) Test02

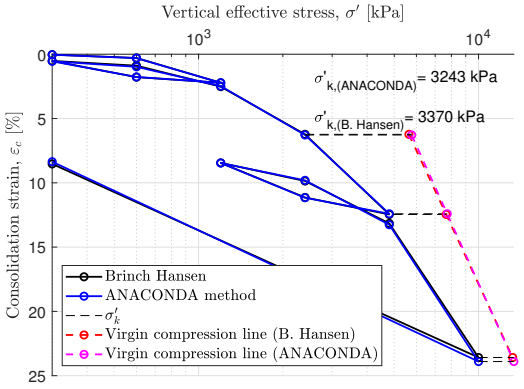

(a) Test03

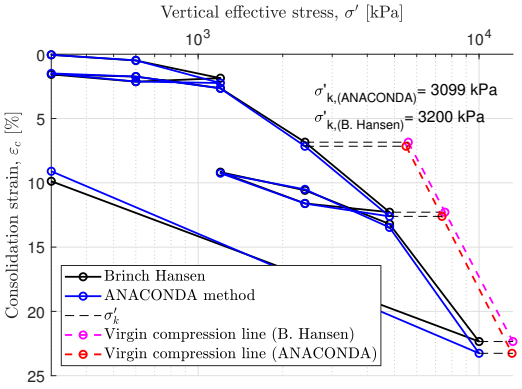

(b) Test04

Methods	Test01 (24hr/load-step)		Test02 (24hr/load-step)		Test03 (14days/load-step)		Test04 (14days/load-step)	
	ANACONDA [kPa]	B. Hansen [kPa]	ANACONDA [kPa]	B. Hansen [kPa]	ANACONDA [kPa]	B. Hansen [kPa]	ANACONDA [kPa]	B. Hansen [kPa]
Janbu	450	450	450	450	483	483	472	472
Pacheco Silva	2508	2676	3053	3087	3088	2985	3240	2936
Jacobsen	4317	4314	5510	5168	6740	6486	6198	6400
Akai	4800-6100	4800-6300	4800-9500	4800-8450	4939-7465	5190-85056	4700-8209	4800-9200

Table D.1: Preconsolidation stress results.